Author for correspondence:
Shoji Takeuchi
e-mail: takeuchi@iis.u-tokyo.ac.jp

†These authors contributed equally to this work.

Membrane protein-based biosensors

Nobuo Misawa[1,†], Toshihisa Osaki[1,2,†] and Shoji Takeuchi[1,2]

[1]Artificial Cell Membrane Systems Group, Kanagawa Institute of Industrial Science and Technology, 3-2-1 Sakado, Takatsu, Kawasaki 213-0012, Japan
[2]Institute of Industrial Science, The University of Tokyo, 4-6-1 Komaba, Meguro, Tokyo 153-8505, Japan

TO, 0000-0003-1659-2541; ST, 0000-0001-6946-0409

This review highlights recent development of biosensors that use the functions of membrane proteins. Membrane proteins are essential components of biological membranes and have a central role in detection of various environmental stimuli such as olfaction and gustation. A number of studies have attempted for development of biosensors using the sensing property of these membrane proteins. Their specificity to target molecules is particularly attractive as it is significantly superior to that of traditional human-made sensors. In this review, we classified the membrane protein-based biosensors into two platforms: the lipid bilayer-based platform and the cell-based platform. On lipid bilayer platforms, the membrane proteins are embedded in a lipid bilayer that bridges between the protein and a sensor device. On cell-based platforms, the membrane proteins are expressed in a cultured cell, which is then integrated in a sensor device. For both platforms we introduce the fundamental information and the recent progress in the development of the biosensors, and remark on the outlook for practical biosensing applications.

1. Introduction

Biological membranes are one of the essential components of living organisms, forming physical boundaries in biological cells, such as the plasma membrane and the organelle membranes. The principal components of membranes are phospholipids and membrane proteins. Phospholipids are amphiphilic molecules consisting of a hydrophilic head group and hydrophobic tails. They form a bilayer-membrane configuration in aqueous environments, which is attributed to the hydrophobic interactions of their hydrocarbon chains. Lipid bilayer membranes function as hydrophobic barriers against soluble and ionic molecules and prevent the entry of such molecules into the cytoplasm and organelles. Membrane proteins are incorporated in the lipid bilayer and allow signal transduction and transport of ligand molecules across the membrane. Because of these functions, membrane proteins account for a significant proportion of pharmaceutical drug targets [1]. The sensory systems of living organisms, which function to detect and respond to various environmental stimuli such as olfaction and gustation, heavily depend on membrane proteins. For example, in the insect olfactory system, the olfactory receptor is considered a ligand-gated ion channel [2,3]. Binding of an odorant molecule to the ionotropic receptor directly triggers the influx of cations into the cell through the membrane; this influx stimulates the neurons. In the mammalian olfactory system, several proteins cooperate and organize the sensing mechanism. The olfactory receptor is a G-protein-coupled receptor (GPCR; GPCRs constitute a large protein family of receptors), and binding of a ligand molecule to the GPCR initiates the second-messenger cascade of olfactory transduction, and finally leads to a cation influx through the ion channel associated with the system [4]. Since these receptors act as ligand-sensing elements, numerous studies have attempted to use this sensing property of the membrane receptors for the development of biosensors. One of the attractive characteristics of biological systems is their specificity to ligands (i.e. target substances), which is considerably superior to that of traditional human-made sensors. Moreover, sensory systems often include a mechanism of input amplification that enhances the output signal-to-noise ratio. Biosensors that embed sensory systems are based on
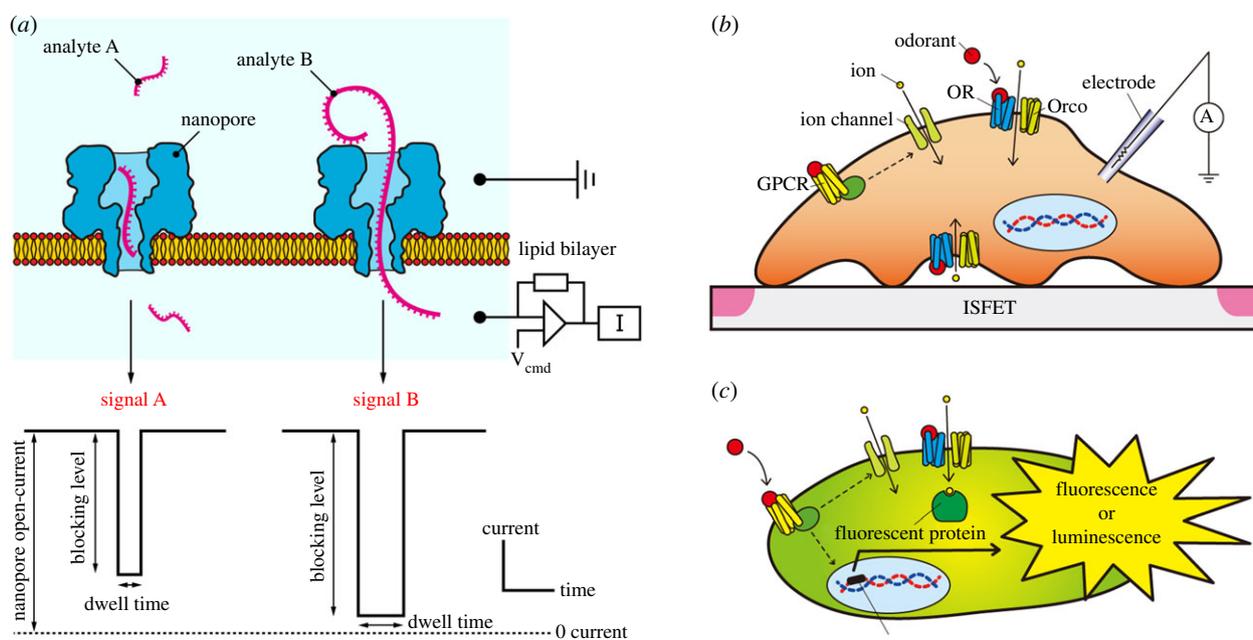
Figure 1. Membrane protein-based biosensors on (*a*) a lipid-bilayer platform and (*b,c*) cell-based platforms. On the lipid bilayer platform, the nanopore protein is incorporated in the lipid bilayer. Single analyte molecules are detected based on the signatures of the current trace that translates the interaction between the analytes and the nanopore. On the cell-based platforms, such as those for odorant sensing, cell responses to odorants can be determined by (*b*) measuring the electrical alterations of the cell using electric signal measuring systems, including ion-sensitive field effect transistor (ISFET), (*c*) detection of fluorescence or luminescence changes initiated by olfactory stimuli. In this case, utilized cells express G protein-coupled receptor (GPCR) or olfactory receptor (OR) with OR co-receptor (Orco). (Online version in colour.)

two major platforms: the lipid bilayer-based platform and the cell-based platform (figure 1).

In this review, we highlight both the fundamental information available and the recent progress in the development of membrane protein-based sensors based on these two platforms, and further discuss emerging issues with the development and application of such biosensors. For the lipid bilayer-based platform, the development of sensing methodologies is classified with their applications while the characteristics and the performance of the cell-based platform systems are described in accordance with the cell species-based classification. Finally, we briefly remark on the outlook of future studies on each platform for practical biosensing applications.

2. Lipid bilayer-based sensors

This section surveys recent progress on the development of bio-sensors based on lipid-bilayer platforms that take advantage of membrane proteins. We especially focus on applications that use electrical detection technologies (figure 1*a*). The membrane proteins spontaneously transduce the binding of the target molecules into electrical signals, where the lipid bilayer membrane forms a bridge between the membrane proteins and the device components. Among the various types of membrane proteins studied, biological nanopores have been extensively explored as a sensor element; this has broadened the potential application of the sensor described below. A suspended lipid bilayer (also known as a free-standing lipid bilayer) serves as an electrical separation between the *cis* and *trans* sides of aqueous electrolyte solutions on the platform. Therefore, the biological nanopore becomes the only pathway between the two aqueous phases separated by the bilayer. Diverse types of lipid bilayer platforms have been developed till date [5–16]. An example is the double-well chip, in which a bilayer

is formed between a pair of aqueous droplets in lipid-dispersed oil [5,6]. The principle of the sensor is similar to that of a Coulter counter, that is the size and the number of analyte molecules are estimated by the blockade events occurring at the nanopore. Under an electrophoretic force, analyte molecules are transported to the nanopore and disturb the ionic current flowing through the pore. Accordingly, the fingerprint of the analyte is reflected in the time-course signature of the ionic current. Basically, the sensors are able to detect single analyte molecules without requiring of labels or tags and will have a potential for rapid, sensitive and portable applications. Here, we discuss such nanopore-based sensors, according to their application. We also briefly remark on the development of synthetic nanopores to be used as sensor elements; this is an emerging area in the development of lipid bilayer-based sensors.

2.1. Mass spectrometry of poly(ethylene glycol)

Mass spectrometry of polydisperse poly(ethylene glycol) (PEG) molecules is a comprehensible example of nanopore-based sensing systems. Kasianowicz and co-workers demonstrated that the nanopore is able to discriminate PEG molecules of different molecular weights with the resolution of the single repeating unit [17]. The system consists of a pore-forming toxin, α-haemolysin from *Staphylococcus aureus* (αHL nanopore) [18], and a lipid bilayer. The αHL nanopore is composed of two parts, an extracellular vestibule and a transmembrane β-barrel (2.5 nm diameter and 5 nm length), connected by a 1.4 nm constriction of the diameter. The nanopore electrically connects the two aqueous phases (*cis* and *trans* sides), in which the conductance is determined by the nanopore dimensions and the electrolyte solution; e.g. αHL nanopore shows 1 nS in 1 M KCl solution at a neutral pH [19]. Driven by a DC electric field (*trans* side positive), the PEG molecules in the *cis* side solution block the nanopore
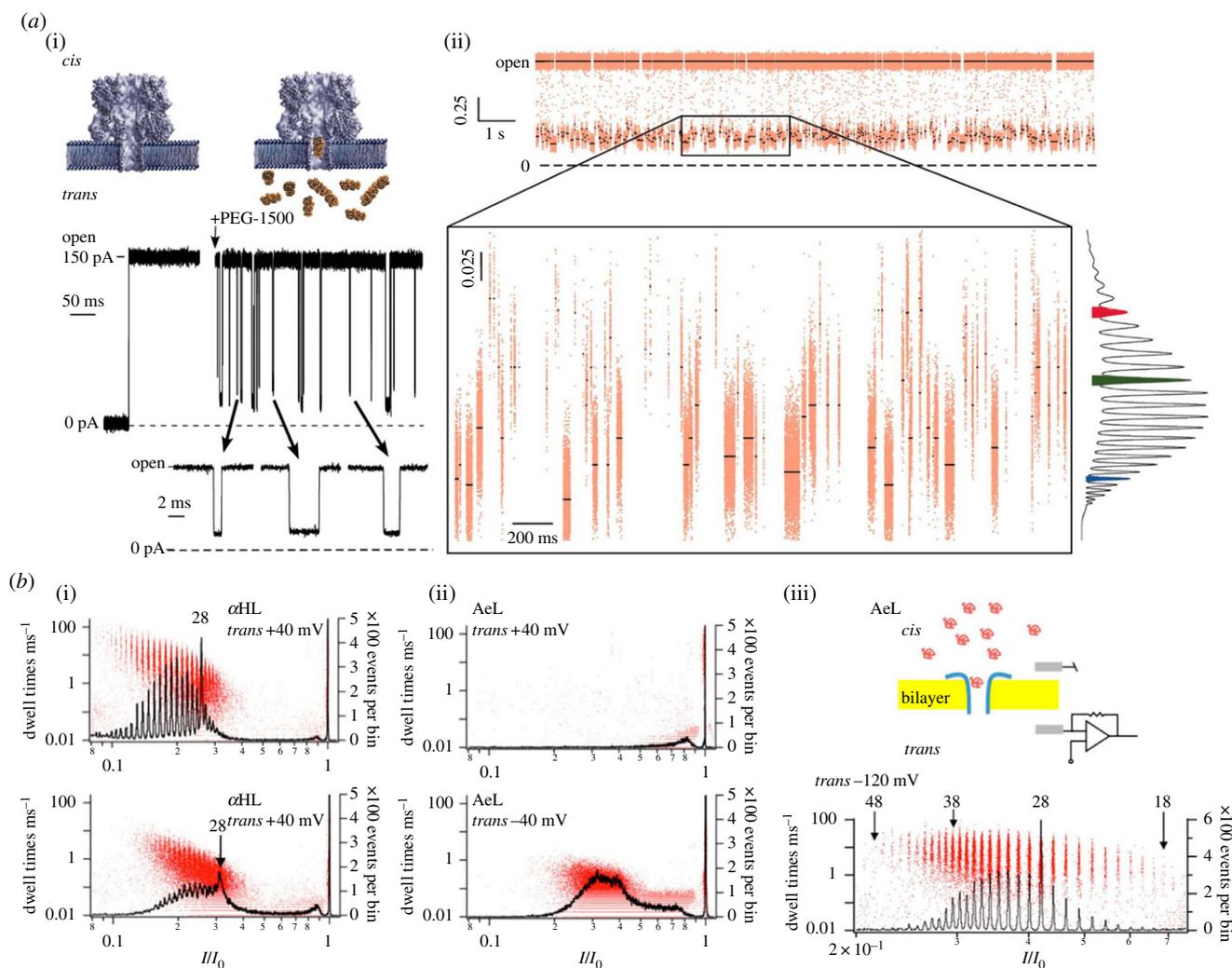
Figure 2. (*a*) Time-course of blocking current caused by non-ionic PEG polymer through a single αHL nanopore (i,ii top). The mean levels of the blocking current generated by individual events (the solid black lines shown in the magnified blockades) resolved the differences in the molecular masses of polydisperse PEG (M_r = 1500 g mol^{-1}) with the resolution of the single repeating unit, as presented in the right histogram (ii). Reproduced with permission from Robertson *et al.* [17] (Copyright © 2007 National Academy of Sciences). (*b*) Histograms of the mean blocking current levels (I/I_0) of polydisperse PEG at *trans* positive and *trans* negative electric fields for αHL nanopore (i) and AeL nanopore (ii,iii), respectively. Red scatterplots represent the dwell times of individual blocking events against I/I_0. The numbers indicated in (iii) represent the repeat units of PEG. Adapted with permission from Baaken *et al.* [20] (Copyright © 2015 American Chemical Society).

one after another, and suppress the open-pore current temporally and partially, depending on the molecular weight (figure 2*a*). The blockade signals are characterized by the conductance level and the residence time. It should be noted that PEG, a non-ionic polymer, strongly interacts with the pore lumen, which extends the dwell time of the blockade events considerably; otherwise, the events would be undetectable at the sampling resolution of the microseconds. By taking the mean conductance value of each blockade event, numerous samplings of the polydisperse PEG (25 < the number of repeat unit < 50) were clearly resolved to the mass spectrum of the different molecular sizes; a larger molecular weight resulted in a deeper blockade level. The mean residence time increased with increasing molecular weight.

The signature of the blockade event considerably changes with the species of nanopores because of the difference in the interactions between the pore lumens and the analyte. The Behrends group compared the mass spectra of polydisperse PEG between the αHL nanopore and aerolysin nanopore (AeL; from *Aeromonas hydrophila*) (figure 2*b*) [20]. Unlike the mushroom-like αHL pore, the AeL nanopore does not possess a vestibule region and forms a rivet-like pore. The transmembrane

part is composed of a heptameric β-barrel with a diameter of approximately 1–1.6 nm, similar to that of the αHL pore [21,22]. Despite the similarity in the pore dimension, the mass spectrum of PEG was obtained only when the *trans* side voltage was negative, which has an opposite polarity to that of αHL. Moreover, the dwell time was less dependent on the PEG molecular weight for AeL than it was for αHL. The results indicate that there were significantly different interactions between the respective pores and PEG. In the AeL pore lumen, 91 charged residues (seven positive and six negative per monomer) form positive and negative rings collaterally [23,24], and this specific charge layout was considered to raise the differences. Although further experimental and theoretical studies are required, this finding implies that the sensor characteristics such as sensitivity and specificity to the analytes could be controlled by coordinating the geometry and electrostatic properties of the pore.

2.2. Nucleic acid sequencing
Nucleic acid analysis is a representative application of lipid bilayer-based sensors using a biological nanopore. The DNA
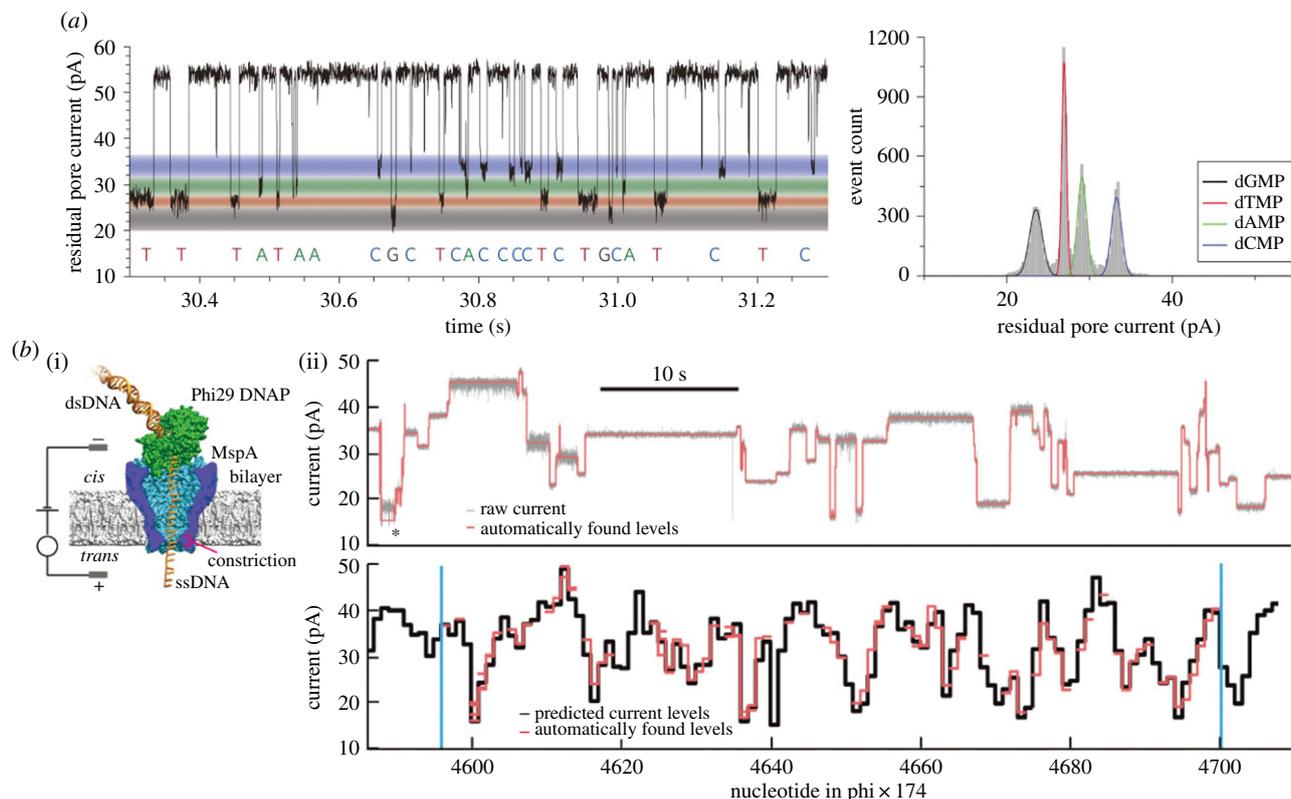
Figure 3. (a) Discrimination of four types of monophosphates (dGMP, dTMP, dAMP and dCMP) using an engineered nanopore coupled with a molecular adapter. Resulting from the interaction with the pore, the monophosphates generated different levels of blocking current, as shown in the right histogram. Reproduced with permission from Clarke et al. [26] (Copyright © 2009 Macmillan Publishers Ltd). (b) DNA sequencing using a MspA nanopore and a phi29 DNA polymerase (i). Blocking levels (pink line) were estimated from a raw current trace (grey line, ii, top), and the levels of the pink line were compared with the predicted levels from the reference sequence (black line, ii, bottom). Mismatches (skipped or multiple-read levels) were found in some parts. Reproduced with permission from Laszlo et al. [27] (Copyright © 2014 Macmillan Publishers Ltd).

sequencing technology using the nanopore was developed by the interaction between the pore lumen and the nucleobases on target DNA. Because they interact differently with the pore lumen, the four nucleobases theoretically show different conductance levels in the blocking current [25,26] (figure 3a). Therefore, it is expected that information of the DNA sequence appears in the time-course of the blocking current when single-stranded DNA (ssDNA) translocates through the nanopore. In principle, labelling or amplification of DNA is unnecessary for nanopore-based sequencing technology. Practically, however, two challenging issues have been addressed and investigated in numerous studies. The first issue was the short dwell time, estimated as $1-10 \mu s$ for each nucleobase. Considering the electrical current noises, it is not realistic to rigorously discriminate between the minute conductance differences caused by single nucleobases in such a short period of time. To extend the dwell time, an enzyme was additionally incorporated into the platform (figure 3b). The enzyme, polymerase or helicase, was coupled to the cis side of the nanopore and played a role of the DNA delivery to the pore from one nucleobase to the next. The DNA translocation was delayed in the range of a few tens of milliseconds per base, which would allow enough data points to each nucleobase for determination of the mean conductance level. The second problem was the pore length where the nucleobases could interact. Since the interaction determines the blocking current level, the pore structure critically affects the sequencing quality. For the αHL pore, approximately 12 nucleobases are considered to interact with the lumen at the β-barrel, indicating that the target current

signal from the single base will be buried by the influences of the other bases. As noted above, the geometry and charge distribution of the pore lumen strongly affects the feature of the lumen–nucleobase interaction. Accordingly, the amino acids on the β-barrel of αHL were carefully engineered one after another to maximize the signal-to-noise ratio [28,29]. The selection of a pore with favourable geometry was an alternative solution for this issue. A mutated form of Mycobacterium smegmatis porin A (MspA) forms a funnel-like nanopore, in which a strong interaction with DNA only occurs at the short constriction with a length of 0.6 nm. Note that αHL consists of a 5 nm long β-barrel. The Gundlach group reported that the MspA nanopore was able to improve the discrimination of the four nucleobases by the blocking current signals [30,31], and successfully demonstrated the sequencing of a bacteriophage phi X 174 genome (4.5 kb) using the MspA pore coupled with a polymerase (figure 3b) [27]. The Church group took a unique approach, using four species of tagged nucleotides in addition to the αHL nanopore and a coupled polymerase. The polymerase synthesizes a complementary DNA strand of the target DNA by using the tagged nucleotides. As growing the DNA, the tagged nucleotide binds with the polymerase while the tag composed of a specific oligonucleotide is captured in the pore, released by the reaction, and generates the nucleotide specific blocking signal. This research group developed the system on a complementary metal oxide semiconductor (CMOS) chip and demonstrated 264 parallel measurements [32,33]. The commercial device, MinION, released by Oxford Nanopore Technologies has promoted

and expanded the advancement of sequencing technologies. Further details of the history and progress of nanopore-based DNA sequencing can be found in recent reviews [34–36].

2.3. MicroRNA diagnosis

Biological nanopores have also been used to detect specific sequences on nucleic acid samples. An example of the application is for liquid biopsy of circulating microRNA (miRNAs; short, non-protein coding RNA composed of approximately 20–30 nucleotides). Mature miRNAs in the cytoplasm are relevant to the regulation of gene expression at the post-transcriptional level [37], and distinct patterns of abnormal miRNA expression have been found in various diseases including tumours [38]. Numbers of miRNA detection methods that use a wide range of analytical technologies have emerged [39]. Nanopore-based sensing systems use complementary sequences of nucleic acids as probes for the detection of target miRNAs. The αHL nanopore of 1.4 nm diameter is adequate for the translocation of single-stranded nucleic acids but undersized for double-stranded forms, thus generating a specific signature of the blocking current in the presence or absence of target miRNA.

One of the most critical and challenging tasks for circulating miRNA detection is ensuring the sensitivity of the sensor because the concentrations of the miRNAs could be as low as a femtomolar. The Gu group proposed a sensitive system using an engineered αHL pore and DNA probe (figure 4a) [40]. The probe consisted of a complementary oligonucleotide with extensions of poly(dC)$_{30}$ at both ends, which enabled the nanopore to trap the probe. The trapping and unzipping of a miRNA-probe hybrid in the pore provided the three-step signature of the blocking current, which corresponded to the trapping and translocation of the probe, the partial blocking with the unzipped miRNA at the vestibule, and the translocation of the miRNA. A concentration gradient or a pH gradient was applied between the *cis* and *trans* side of the KCl electrolyte solution to enhance the frequency of the translocation events [42–45]. While the frequency of the miRNA-probe translocation is proportional to the miRNA concentration, a sufficient number of events (e.g. a few hundred) is required for the quantitative estimation even at a very low miRNA concentration. By using the 0.2 M/3 M (*cis/trans*) condition, Gu *et al*. reduced the limit of detection to sub-picomolar concentrations [40]. The de Planque Group further examined the frequency and the dwell time of the translocation event under asymmetric conditions of both electrolyte species and concentrations [46]. In the presence of a KCl gradient of 0.5 M/4 M (*cis/trans*), the event frequency increased by approximately 60-fold compared to that with the symmetric 1 M KCl, because the electrophoretic force close to the pore was larger. The dwell time was moderately extended by replacing the symmetric KCl with LiCl/KCl (*cis/trans*), allowing the identification of the blocking current signature. Kang and colleagues showed the potential usefulness of tetramethylammonium chloride (TMA-Cl) instead of KCl, which enhanced the event frequency and prolonged the dwell time simultaneously [47]. Anions may also affect the characteristics of the translocations as reported by Bezrukov and colleagues [48]. The behaviour of channel-forming peptide gramicidin A (gA) in a lipid bilayer showed a good correlation with the anion position in the Hofmeister series. The open-channel conductivity increased twofold in the order of the ranking from

kosmotropic to chaotropic anions, and the dissociation kinetics of the gA channel was similarly delayed 20-fold, where the anions were considered to interact with the lipid bilayer as well as the gA channel. As mentioned above, the nanopore-sensing method uses stochastic single-molecule capturing at the pore. For the quantification of the analyte concentration, accumulation of the sensing events is necessary, i.e. the method relies on a series of stochastic phenomena. Accordingly, the quantification becomes extremely difficult at ultra-low concentrations such as femtomolar. To overcome the limitation, Kawano and colleagues combined the nanopore system with a 1 h isothermal amplification technique to enhance the input signal with the aid of a biological technique and demonstrated the detection of 1 fM miRNA [49].

In addition to the sensitivity, specificity to a target miRNA is mandatory for miRNA diagnosis in the presence of miscellaneous nucleic acids in a biopsy sample. The Gu group designed a peptide nucleic acid (PNA) with extension of a polycationic peptide at the N-terminus as a probe (figure 4b) [41]. Upon hybridization, the miRNA-PNA probe formed a dipole complex (positive and negative charges at each side). The sample and probe were infused at the *trans* side of the aqueous solution, and a DC electric field was applied as the *cis* side negative. The electrophoretic force allowed only the miRNA-probe hybrid to move toward the pore and the other nucleic acids were repelled from the pore. Because PNA-RNA hybrids are energetically more stable than DNA-RNA hybrids, a single mismatch of a PNA-RNA presents a larger energy loss than that of a DNA-RNA [50]. This large destabilization allowed the detection of the single mismatch on the PNA-RNA hybrid by the current signals and, thus, enabled the discrimination of single nucleotide-difference from the target miRNA. For the discrimination of the single nucleotide mismatch, Wang and colleagues used a locked nucleic acid (LNA) probe [51], which is a nucleic acid analogue bridging between 2′ oxygen and 4′ carbon that significantly stabilizes the hybridization. Similar to the PNA-RNA, the LNA probe was able to discriminate a single nucleotide difference on a miRNA from the differences of the blocking dwell times. It is worth digressing briefly to state that the White group reported the identification and discrimination of mismatched base pairs and epigenetic modifications on DNA [52,53]. They used latch constriction in the vestibule of the αHL nanopore. The mismatch and epigenetic modifications caused different signatures on the time-course of the blocking current: two or three conductance levels with specific transition kinetics due to the interactions of the nucleotide with the residues at the constriction. The work indicates a lack of understanding of the behaviour of nucleic acids in the nanopore and the potential for discovery and development of nanopore technologies.

For the practical use, a pattern of multiple miRNAs must be quantified for the accurate diagnosis of a disease. Multiplex miRNA detection was demonstrated using a PEG-tagged DNA probe [54]. Each probe consisted of a complementary part and a 3′-poly(dC)$_{30}$ extension where a specific length of PEG (0 to 24 mer) was covalently linked as a side branch using click chemistry. The PEG tags additionally suppressed the blocking current during the translocation of the probe, depending on the PEG length, allowing the discriminations of multiple miRNAs based on the depth of the current level. They demonstrated that the concentration of the target miRNA was proportional to the event frequency and unaffected by the coexisting miRNA-probe hybrids [54].
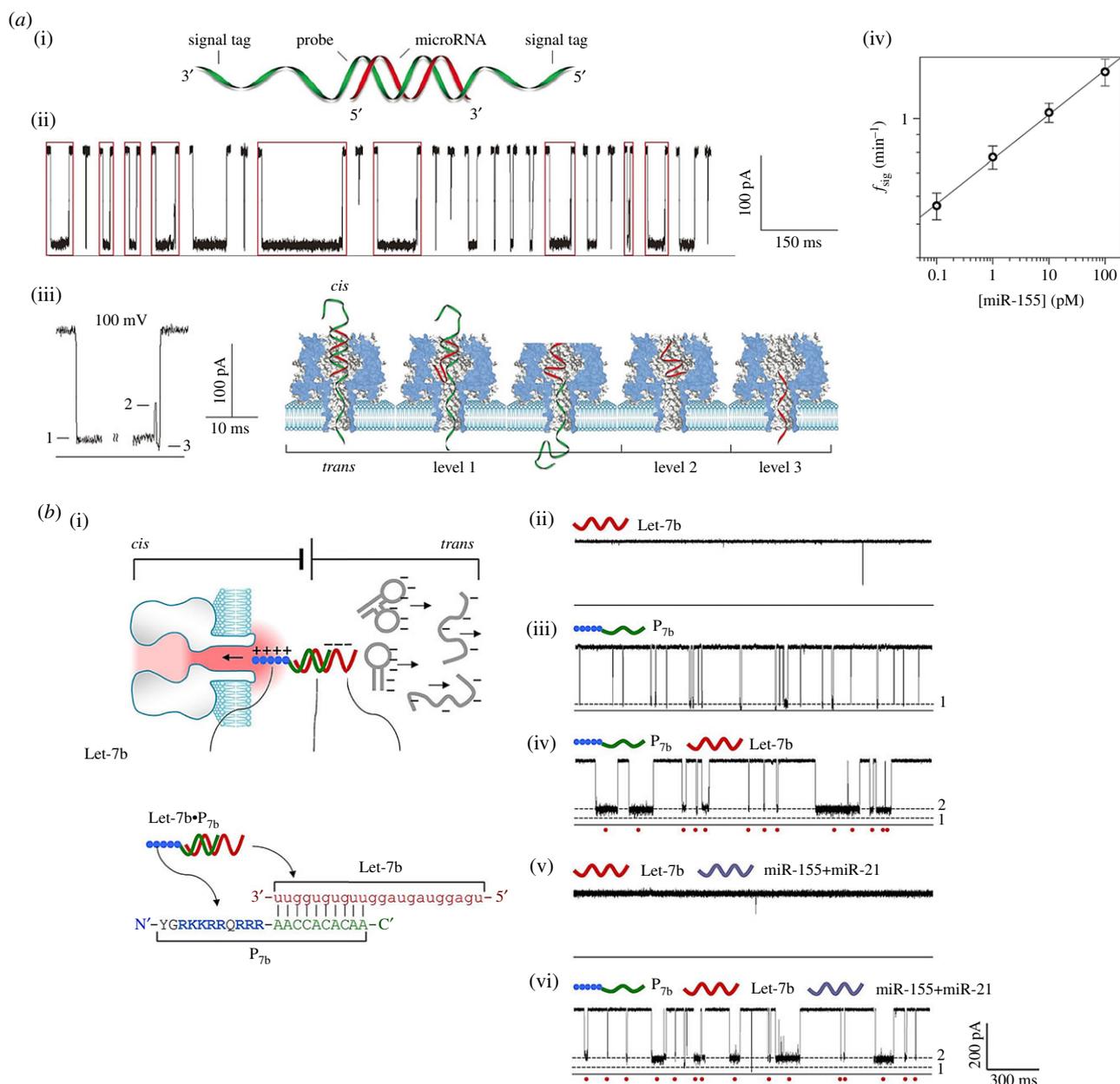
Figure 4. (a) Detection of miRNA using a complementary DNA probe with a nanopore. Schematic of miRNA bound to the probe (i). Translocation of the miRNA-probe hybrid through the nanopore generated the three-step signature on the blocking current (ii,iii). The numbers in a2 indicate the levels in a3. The concentration of miRNA was quantified using the frequency of the three-step signatures appeared (iv). Reproduced with permission from Wang *et al.* [40] (Copyright © 2011 Macmillan Publishers Ltd). (b) Detection of a specific miRNA in the presence of miscellaneous nucleic acids. The PNA probe conjugated with a polycationic peptide allowed the delivery of the target miRNA to the pore under the influence of the electrophoretic force (i). Only the miRNA-probe hybrid was trapped and produced the shallow and long blocking signature referred as level 2 (ii−vi). Adapted with permission from Tian *et al.* [41] (Copyright © 2013 American Chemical Society). (Online version in colour.)

2.4. Chemical and biomolecular sensing

Biological nanopores have also been used as sensors for organic compounds and biomolecules including peptides and proteins [55–60]. Thus, diverse applications are expected in the field of medicine, food production, cosmetics, agriculture and farming, and environmental concerns, as well as safety and security.

The technologies presented above show the future potential for the identification of epigenetic modification or single nucleotide polymorphism on DNA using the nanopore-nucleic acid interaction [52,53,61,62]. In addition, the nanopore coupled with a complementary DNA would facilitate the early detection of pathogenic DNA, shown in the detection of the anthrax-related DNA of *Bacillus anthracis* [63]. Not only nucleic acids, but short peptides are also able to translocate

through the nanopores, in which the fingerprints of the peptides are reflected in the blocking current signatures as a result of the interaction with the pore. For example, the form of amyloid beta (Aβ42; involved in Alzheimer's disease) was distinguished using the αHL pore [64]. Since Aβ plaques are found in the brains of Alzheimer patients, the aggregation process of the Aβ peptides was monitored in real time by analysing the frequency and conductance levels of the blocking events. Moreover, a botulinum neurotoxin (BoNT; the most acutely lethal toxin known, which causes botulism) sensor was developed by detecting a peptide digested by the toxin's enzymatic activity (figure 5a) [65]. The system consisted of the AeL nanopore and the synaptic protein as the probe, which is the substrate of the digestion. The presence of the BoNT type B cleaved the probe protein and produced a short
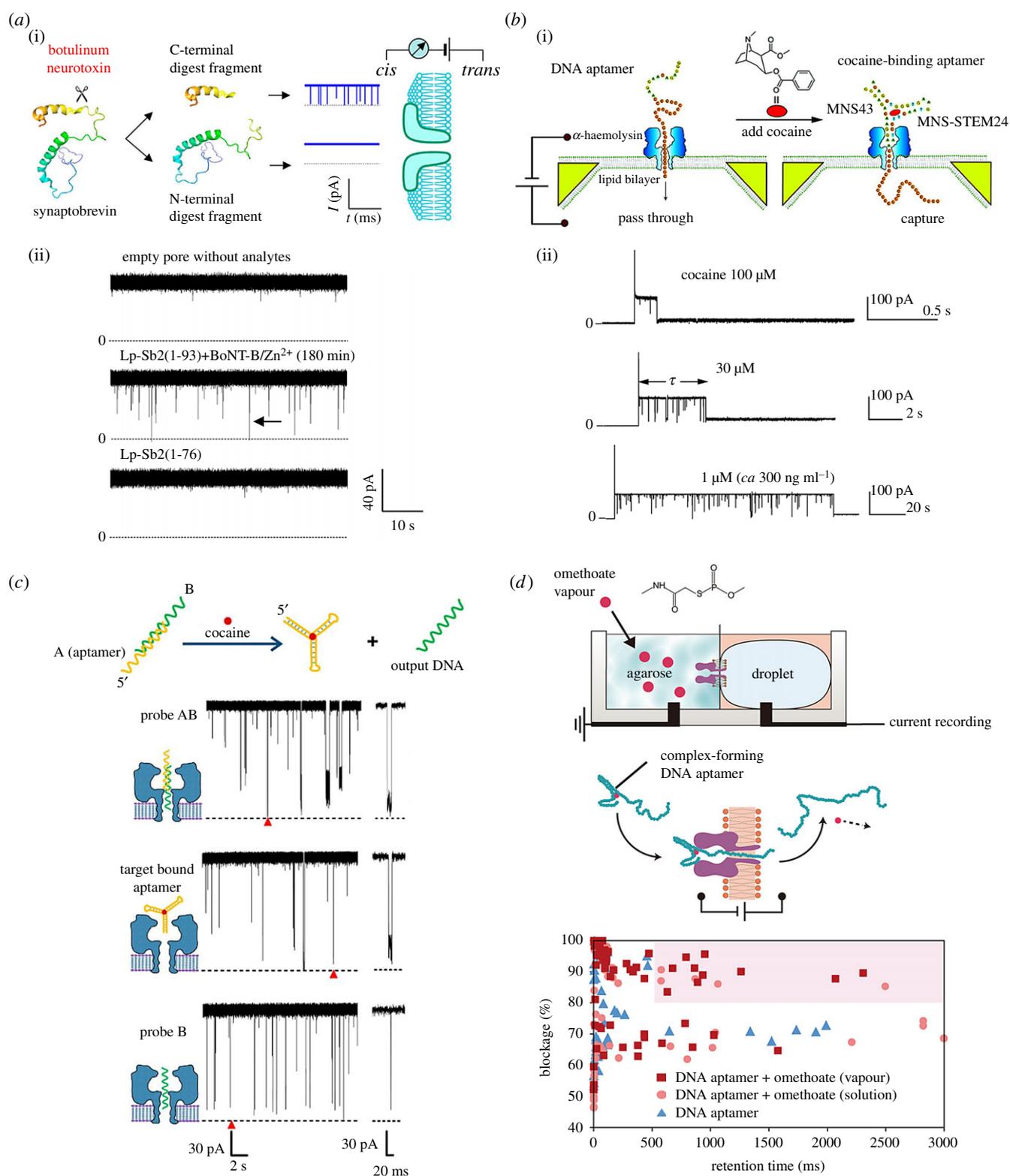
Figure 5. (a) Detection of botulinum neurotoxins (BoNT type B) by using its own enzymatic activity. The probe, a synaptic protein, was cleaved by BoNT, and the product, C-terminal fragment, was detected by AeL pore (i). Blocking current signals were observed in the presence of the BoNT (middle trace), whereas the N-terminal fragment (Lp-Sb2(1-76)) did not interact with the pore (bottom trace) (ii). Adapted from Wang *et al.* [65] (Copyright © 2011 American Chemical Society). (b) Detection of a cocaine molecule with the aid of DNA aptamer (i). Because the aptamer strongly bound to the target molecule, the complex clogged at the αHL pore and generated a blocking current for a long duration (ii). The interval time (τ) was statistically increased with decreasing cocaine concentration. Adapted with permission from Kawano *et al.* [66] (Copyright © 2011 American Chemical Society). (c) Cocaine detection in biological fluids using a pair of DNA probes: cocaine aptamer (A, yellow) and a reporter (B, green) that is partly complementary to the aptamer. Without cocaine, the DNA probe blocked the nanopore with long duration (top trace). With cocaine, the cocaine-aptamer complex showed long blockades (middle trace), while the reporter provided the translocation event with a short blocking current signature (bottom trace); the signals indicated with the red arrowheads were expanded in the right side of each trace. Adapted with permission from Rauf *et al.* [67] (Copyright © 2017 American Chemical Society). (d) Pesticide vapour detection using a nanopore sensing system. Pesticide vapour (omethoate molecule) absorbed in the agarose gel, formed a complex with its aptamer, and was translocated through the pore by an electrophoretic force (top, middle). Blocking current level against the retention time for individual translocation events (bottom). In the presence of omethoate, the deep and long blocking signature was apparent (shaded with pink). Adapted with permission from Fujii *et al.* [68] (Copyright © 2017 The Royal Society of Chemistry).

peptide, which was detected by the current signals. Alternatively, the pore was insensitive to the proteins and serum components contained in the samples. Sub-nanomolar concentrations of the BoNT type B were reportedly identified in the order of minutes by the system.

To deal with diverse molecular targets, engineered nanopores and supplementary molecules have been introduced. The Bayley group discovered a strong interaction between nitroaromatic molecules and a ring of aromatic amino acids located near the constriction in a mutant αHL pore [69]. The aromatic–aromatic interaction in the pore exhibited a long dwell time on the blocking current signature for the nitroaromatics, including 2,4,6-trinitrotoluene (TNT) and, thus, is considered a useful sensor element for explosives in industrial and military use. Similarly, nitrogen mustards, known as chemical warfare agents, were detected using an engineered αHL nanopore [70]. In this case, a cysteine residue was introduced near the constriction of the αHL pore. The thiol group of the cysteine residue covalently reacted with the chloroethyl group of the mustards under basic conditions, generating a stepwise blocking signal depending on the number of captured mustards at the pore. As a supplementary molecule, β-cyclodextrin (βCD) was initially used to support the function of the nanopores. Because of its size, βCD temporarily lodges into the αHL nanopore from the *trans* side and becomes a hydrophobic cavity for various small organic molecules (Mw ~300) [71]. Similar to the relationship between the nanopore and analytes, the interaction between the βCD cavity and the organic molecule determines the signature of the blocking current. The reactivity of βCD can be adjusted by chemical modification of the cavity of βCD, which expands the sensing specificity as well as the range of the analyte [72].

Alternative supplementary molecules used are aptamers consisting of short, single-stranded oligonucleotides or peptides. Because of the designed sequences, aptamers bind to various molecules with high specificity and affinity, called chemical antibodies [73]. The Takeuchi group introduced a pair of DNA aptamers as a probe that binds to a cocaine molecule for the rapid detection of illegal drugs (figure 5*b*) [66]. Since the aptamers were designed to be unfolded in the absence of cocaine, spike-like blocking signals were observed under a DC electric field (*cis* side negative) due to the translocations of the aptamers. In the presence of cocaine, the aptamer formed a cocaine–aptamer complex that clogged the αHL pore and generated a deep blocking signal that lasted until the DC field was turned off. The system was able to detect $300 \, \mathrm{ng \, ml}^{-1}$ of cocaine (the cut-off value for drug tests) within 60 s, and distinguished cocaine from aminobenztropine (a cocaine analogue), facilitated by the affinity and specificity of the aptamer. For quantitative assays, a reporter DNA, which was partly complementary to the aptamer, was additionally incorporated into the system [74]. The aptamer was pre-hybridized with the reporter DNA, while the hybrid was unwound by the presence of the target molecules and displaced to the target-aptamer complex and the released reporter. In this system, the translocation events were attributed to the reporter DNA; thus, the event frequency was proportional to the concentration of the target molecules. Wu *et al.* further integrated a magnetic-bead technique to eliminate the interference of the target-aptamer complex and succeeded in detecting vascular endothelial growth factor (VEGF) at a picomolar order. Using a similar aptamer-reporter system, Li and colleagues performed cocaine detection in human saliva and serum

(figure 5*c*) [67]. Surprisingly, the event frequencies (i.e. the concentration of cocaine) in the biological fluids were almost consistent with that in an aqueous buffer where 50 nM cocaine was detected in 15 min, which demonstrated the potential of this sensor for practical use. In attempts to further expand the versatility of nanopore sensors, Fujii *et al.* developed a gas absorption system on their lipid-bilayer platform for detection of volatile organic compounds (VOCs) (figure 5*d*) [68]. VOCs, such as odour molecules, include both natural and synthetic chemicals that strongly affect both humans and the environments and, thus, constitute a large proportion of analyte candidates for sensors. An agarose hydrogel, a mucus-membrane mimic, was introduced for effective VOC absorption by direct exposure to the air. The absorbed VOC was bound to the aptamer, and the electrophoretic force transferred the VOC-aptamer complex to the nanopore on a planar lipid bilayer. Pesticide vapour was chosen as a VOC sample, and the signature of the nanopore blocking current was outlined in the presence of the pesticide–aptamer complex. The developed system was able to detect 100 ppb of pesticide in a few minutes after a 10 min exposure of the hydrogel to the pesticide vapour [68]. The feasibility of detecting VOC samples, in addition to the liquid form, would expand the application field of nanopore sensing to other uses such as for fragrances in food products and cosmetics, aerial environmental pollutants, explosives in safety/security and biomarkers in healthcare.

We introduced a few chemical sensors using βCD and aptamers. In the sensing mechanism, these supplementary molecules supported or substituted the recognition role of target analytes with the desired specificity and affinity. Consequently, the sensors are now suitable for use with diverse analytes although the pore lumen does not interact with the analytes. Note that the interaction between the pore lumen and the analyte was the critical factor in the development of mass spectrometry and nucleic acid sequencing. Accordingly, synthetic pores have been reported in recent studies to overcome the limited variations of the pores based on the pore-forming toxins. A peptide nanopore, gA, was partially modified as a semi-synthetic pore, and it revealed the significant influence of the C- and N-termini on the pore properties [75–77]. Using the DNA origami technology, DNA was assembled into sophisticated nanopores with a gating mechanism, functionally resembling ligand-gated ion channels [78–81]. A fully designed metal-organic polyhedral pore or amphiphilic molecules were recently incorporated in a lipid bilayer, and those pore properties were characterized [82–85]. The carbon nanotube (CNT) is another candidate of designed nanopores [86,87]. For larger size analytes such as proteins, Mayer and colleagues developed a solid-state nanopore with a size of few tens of a nanometre, coated with a lipid bilayer on its surface [88]. The analyte proteins were tagged to the lipid bilayer, delivered to the pore, and their shapes and volumes were characterized [89]. We consider that these highlighted studies on various materials would lead to tailor-made nanopores for a broad range of sensing targets.

3. Cell-based sensors

Studies related to cell-based chemical sensors were mostly conducted from the late 1980s to 1990s [90–93]. Since the beginning of the 2000s, the development of cell-based odorant sensors has particularly advanced [94,95]. The detection of

sensor principles is based on the responses of cells to chemical stimuli. There are mainly two types of technologies of cell-based sensor transducer, which are based on the detection of electrical alteration and fluorescence or luminescence emissions as schematically shown in figure 1b,c. The sensor cells are generally spread on electric device or Petri dish at random. There are some reports of cell-array or cell-patterning based on microfabrication technologies [96–98]. Currently, there are numerous cells which maintain the self-contained vital activities such as protein expressions and cellular divisions under a suitable cellular environment. Hence, by creating conditions that ensure cell survival, we can use single cell or cell groups as sensing elements. More specifically, for the sensor cells, harmful substances and contamination by different cells must be avoided. Thus, sterilization is indispensable for preparation of cell-based sensors. Cell-based biosensors, unlike lipid bilayer-based sensors, require the preparation of safe and compatible transducer interfaces for cells. Several examples of odorant sensors using cells expressing olfactory receptors are outlined in the following sections.

3.1. Olfactory sensory neuron or olfactory receptor neuron

Olfactory sensory neurons (OSNs) or olfactory receptor neurons (ORNs) are superficial nerve cells that transfer odorant stimuli to the brain. OSNs express olfactory receptors on the cilia or dendrites, which are close to ambient air in the smell-related organs of organisms [99,100]. The surface of nerve cells contacts odorant molecules through the nasal mucosa or sensillum lymph. As cell-based odorant sensors, OSNs are mostly used in native cells immersed in culture medium that mimics the living system. The application of physiological tissues, including olfactory epithelium, in odorant sensors has been actively studied [101–106]. In terms of cell-based sensors, odorant sensing based on isolated OSNs are presented in this section. The principles of odorant sensing using the responses of OSNs to odorant stimuli can be classified into two groups. One is based on a fluorescent detection method using Ca^{2+} indicators expressed in OSNs, and the other is based on electrical measurements of extracellular membrane potential changes in native OSNs. As detectors, the fluorescent-based method requires a fluorescence measurement system such as fluorometric imaging plate reader, whereas the latter method is exemplified by an electroantennogram (EAG) that directly detects the action potential of OSNs in vivo, and cultivation of OSNs on a metal oxide semiconductor have been reported as described below.

Using a fluorescent indicator for Ca^{2+} in OSNs, four different fruity/floral smells (vanilla, rose, berry and banana) were simultaneously distinguished using the responses of approximately 3000 OSNs isolated from a mouse [96]. The approach was based on the fluorescent analysis of numerous of OSNs, which were arrayed in a microfluidic chamber. Instead of native OSNs, the use of odorant sensors produced by coexpressing insect pheromone receptors and fluorescent indicator for Ca^{2+} in dissociated neural rat cultures have also been reported [107]. This genetically modified system has advantages of easy functional expression of olfactory receptors, prolonged lifetime, and amplification of the weak ionic currents of olfactory receptors.

The application of EAG to the antennae of the blowfly (Calliphora vicina) revealed that OSNs in insect antennae are specifically sensitive to 1,4-diaminobutane, hexanol-1, and butanoic acid [108]. The EAG results also implied that a higher amount of odorant substances saturated the corresponding OSN response. Based on this sensing system, the same research group developed odorant biosensors using other insects, mosquitoes (Aedes comunis), pine weevils (Hylobius abietis) and trogossitid beetle (Trogossita japonica) [109]. In addition, two typical explosives, cyclotrimethylenetrinitramine (RDX) and TNT, were also detected using the EAG system of the rat olfactory mucosa [110]. The use of a microelectrode array (MEA) integrated with a gas intake apparatus to detect the response of cultured OSNs responses on a chip was reported [111]. In that system, limonene and isoamyl acetate odorants were tested, and the firing spikes of the OSNs were investigated by sorting the different spikes from some neuron recordings. A light-addressable potentiometric sensor (LAPS) is applicable for monitoring the extracellular potential changes in OSNs [112,113]. In the LAPS device, OSNs can be cultured on the surface of sensor chips for one week. CMOS can also be used for the detection of action potentials from OSNs cultured on a CMOS chip integrated to a perfusion system [114]. Since MEA, LAPS and CMOS technologies are physically non-invasive measurement systems for cells, they appear to be suitable for prolonged culturing of OSNs.

3.2. Human embryonic kidney cell

Human embryonic kidney (HEK) cells are frequently used for foreign gene expression owing to their high transformation efficiency [115–117]. Some studies have constructed expression system consisting of olfactory receptors in HEK cells and used them for odorant sensing. For the detection of the responses of HEK cells to odorants, surface plasmon resonance (SPR), quartz crystal microbalance (QCM), a fluorescent detection method, and some electrical measurement techniques have been used as transducers of the odorant sensors.

An odorant sensor for octanol detection using QCM and HEK cells expressing the rat olfactory receptor, ORI7, has been reported [118]. Using the ORI7 expressing cell line, the same research group showed that the transformed HEK cells could be used for odorant sensing in combination with several other transducers or detection methods. They used an intracellular Ca^{2+} sensing molecule (yellow cameleon-2), planer microelectrodes, SPR, and cAMP response element reporter assay [119–121]. In addition, the transformed HEK cells were used to demonstrate SPR-based real-time monitoring of five different odorants (heptanal, octanal, nonanal, decanal and helional) [122]. Furthermore, four different kinds of human olfactory receptors, hOR3A1, hOR1A1, hOR1D2 and hOR1G1, are available for odorant detection using HEK cells [123]. The HEK cells expressing each hOR were cultured in microwells constructed of polyethylene glycol diacrylate, and the cells responses to odorants were investigated using fluorescent observation.

Instead of a fluorescent detection method, an extracellular field potential recording is also useful for monitoring of cells responses to several chemical stimuli. Spheroids of HEK cells expressing insect olfactory receptors (GPROR2 from Anopheles gambiae and Or47a from Drosophila melanogaster) were demonstrated for the detection of chemical vapours (2-methylphenol and pentyl acetate) based on electrophysiological measurements [97]. As shown in figure 6, the HEK spheroids were arrayed in an agarose gel microchamber, and a probe electrode
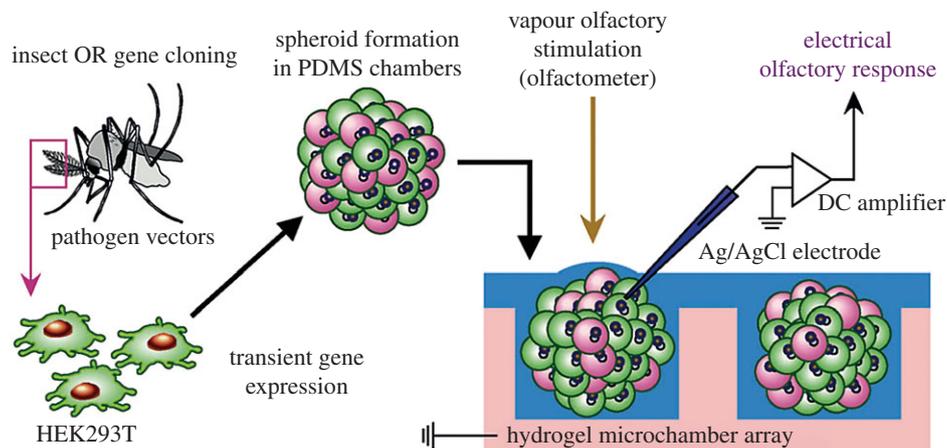
Figure 6. Insect olfactory receptor (OR) and OR co-receptor (Orco) were expressed in human embryonic kidney (HEK) cells that subsequently formed spheroids in polydimethylsiloxane (PDMS) chambers; the spheroids were finally placed into a hydrogel microchamber maintaining the desired moisture conditions. The extracellular field potential of the HEK spheroid was recorded using an amplifier. In this system, the blowing of vapour phase odorants was performed using an olfactometer. Reproduced with permission from Sato & Takeuchi [97] (Copyright © 2014 John Wiley and Sons). (Online version in colour.)
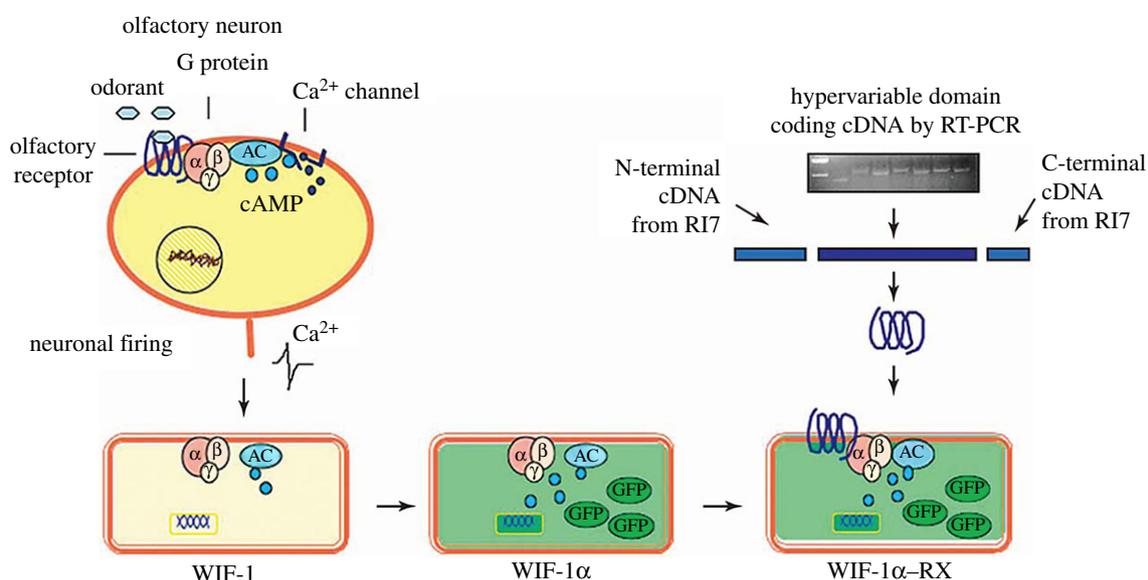
Figure 7. Schematic view of a genetically modified yeast strain (WIF-1α − RX) constructed to produce the odorant sensitive *Saccharomyces cerevisiae*. Except for the olfactory receptor (OR), the olfactory signalling components were cloned and conclusively coexpressed with green fluorescent protein (GFP) and engineered G protein-coupled receptor (GPCR). Reproduced with permission from Radhika *et al.* [130] (Copyright © 2007 Macmillan Publishers Ltd).

was inserted into the intercellular space of the spheroid. Owing to the hydrogel chamber, the system maintained the wet conditions and formed a thin water layer on the surface of spheroids. Consequently, the spheroids were close to the air–water interface, and gas phase odorants could easily access the olfactory receptors from the ambient air.

3.3. *Saccharomyces cerevisiae* (yeast)

Similar to HEK cells, yeasts are also commonly used eukaryotic cells for expressing several proteins [124,125]. In particular, *Saccharomyces cerevisiae* is a representative budding yeast used for forced protein expression [126,127]. This cell strain has been widely used as a model eukaryotic cell in biology and, thus, genetic engineering techniques for yeast have been developed. However, the application of engineered yeast in odorant sensors is much less common presently.

As odorant sensors, the detection methods for the responses of yeast to odorant stimuli are mainly based on fluorescent detection methods. Specifically, responses of the rat ORI7 or OR17-40 expressed in *S. cerevisiae* to heptanal, octanal, nonanal and helional were studied using a G_α subunit-related luciferase luminescence assay [128,129]. Using more elaborate inheritable genetic modification, unnatural olfactory receptors could be expressed in *S. cerevisiae* [130]. They were produced by modifying the ligand-binding site of the rat ORI7. In the study, several odorants (octanol, octanal, heptanal, hexanal, isoproterenol, vanillin, citronellal and 2,4-dinitrotoluene) were tested, and the odorant responses were investigated using a Ca^{2+}-related fluorescent detection system with green fluorescent protein (figure 7). In recent years, to improve the sensitivity of olfactory receptors expressed in *S. cerevisiae*, the coexpression of odorant-binding and receptor-transporting proteins were studied [131]. Such accessory proteins coexpressed with olfactory receptors

appear to affect cell-based odorant detection. In the case of electrical measurements, it is was reported that some *S. cerevisiae* expressing human OR17-40 were immobilized on the microelectrodes, and the responses to helional were detected through conductance changes [132]. Yeast cells were immobilized on gold electrodes by electrostatic binding between the cells and poly-lysine-coated electrode surfaces.

In applications of cells expressing olfactory receptors for odorant sensing, the vertebrate olfaction system was mostly used in *S. cerevisiae* cells similar to that in HEK cells. Compared with invertebrates, vertebrates have numerous molecules or substances for intracellular olfactory signal transduction [133–135]. Therefore, the olfactory system of vertebrates offers more choices for intracellular factors for odorant monitoring than that of invertebrates. In contrast, the constructions of vertebrate olfactory systems using host cells is a comparatively laborious process. Insect olfaction, which is a simpler system than that of vertebrates, is currently attracting considerable attention for use as odorant sensors. In the next section, several research studies using insect olfactory receptors for cell-based odorant sensing are highlighted.

3.4. *Spodoptera frugiperda* cell

The *Spodoptera frugiperda* (Sf) cell, one of the cultured insect cells, is derived from the pupal ovarian cells of the noctuid moth, *S. frugiperda*. It is generally noted that Sf21 cells and the substrain Sf9 cells are frequently used for biological experiments [136]. For cell engineering, Sf cells especially have excellent properties of (i) stable integration with heterologous protein genes into genomes and (ii) can be cultured at room temperature without CO_2 gas. Thus, Sf cells are suitable for use in odorant sensing with cellular expression of olfactory receptors.

Sf21 cells expressing the silkmoth, *Bombyx mori*, pheromone receptor (BmOR1 and BmOR3 that are sensitive to bombykol and bombykal, respectively), with Ca^{2+} indicator protein (GCaMP), were demonstrated as an odorant sensor [137]. The Sf21 cells were introduced into a transparent microfluidic channel device and immobilized in the fluidic channel. Consequently, the fluorescent intensity changes caused by the cell responses to the pheromones could be observed using fluorescent microscopy. Although there was individual cellular variability in the responses to target pheromones, this drawback was resolved by using the region of interest in acquired fluorescent images. In this study, long-term freeze preservation of the Sf21 cells was tested, and the cells maintained their responsiveness to target ligands after two months. The long lifespan of this cellular system demonstrates a breakthrough for cell-based odorant sensing technology. Using the same Sf21 cells mentioned above, this research group also produced other olfactory receptors (Or13a and Or56a derived from *Drosophila melanogaster*) and demonstrated the detection of four kinds of chemicals (bombykol, bombykal, octenol and geosmin) [98]. They regionally immobilized each Sf21 cell group expressing each receptor to four regions on a modified glass substrate and measured the cell responses by fluorescent observation of GCaMP6s in a single visual field (figure 8). This approach showed odorant-specific response patterns to both odorant mixtures and single odorant stimuli. The expandability of this multiple odorant sensing based on a two-dimensional pattern of cell groups depends on a resolution of the patterning and, therefore, the strategy would be difficult with an enormous number of olfactory receptor types.
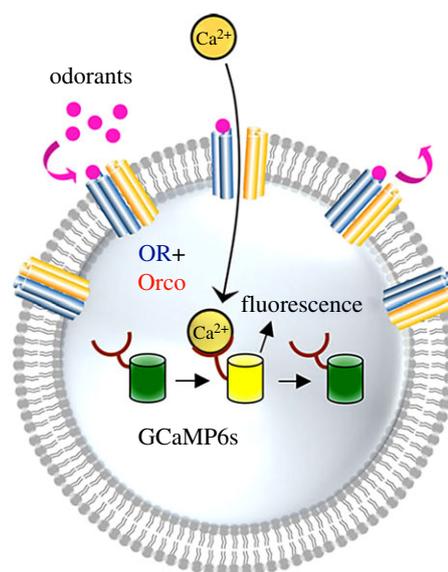

Figure 8. Illustration of odorant detection mechanism in the established odorant sensor *Spodoptera frugiperda* (Sf) cells. The Sf cells express an olfactory receptor (OR), OR co-receptor (Orco), and the fluorescent Ca^{2+} indicator protein GCaMP6s. Reproduced with permission from Termtanasombat *et al.* [98] (Copyright © 2016 Springer Science+Business Media). (Online version in colour.)

To achieve the high-density integration of detection elements for cells expressing diverse olfactory receptors, the application of field effect transistor (FET) to Sf21 cells was recently proposed [138]. The transfected Sf21 cells expressing BmOR3 or Or13a receptors were successfully seeded sparsely on an aluminium extended-gate electrode of the FET. Changes in the drain current implied that the odour-sensitive FET responded specifically the correspondent odorants. In this system, since no fluorometric detection system and invasive electrodes for cells are not required, this electrical measurement approach is expected to be a prospective cell-based integrated odorant sensor for long-term use.

In the construction of expression systems to obtain olfactory receptors using cultured cells, insect olfaction systems are emerging as important cell-based odorant sensing. Concerning expression systems of insect olfactory receptors, other host cells of a different species have also been used in cellular electrophysiology.

3.5. *Xenopus laevis* oocyte

Oocytes of the African clawed frog (*Xenopus laevis*) have been frequently used as expression cells for numerous years in the functional analysis of membrane proteins including several olfactory receptors [139–141]. In contrast to generally cultivated cells, *Xenopus* oocytes are immature egg cells, and they are surgically harvested from the ovaries of living *X. laevis* to obtain the cells in each case. *Xenopus* oocytes are very large with single cells that are approximately 1 mm in diameter. Hence, they are easy to handle for gene injections and electrical measurements using glass capillaries. *Xenopus* oocytes have recently been tested for use as a chemical sensor element and not only as an analysis object in electrophysiological studies. For the application of *Xenopus* oocytes as chemical sensors, footprint downsizing of the measurement system has been attempted.
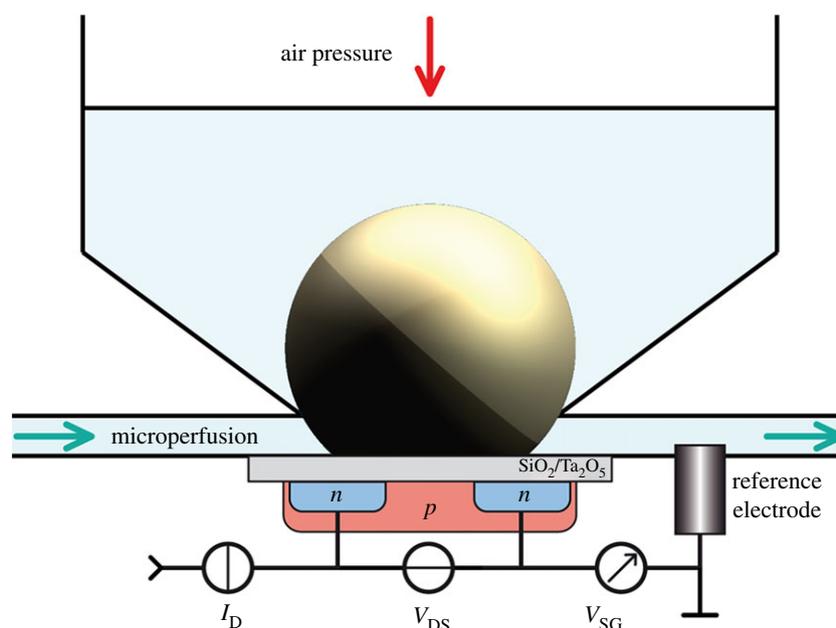
Figure 9. Schematic image of the cross-section of a device with a *Xenopus* oocyte on the surface of an *n*-channel field-effect transistor (FET). The oocyte is held down on the sensitive layer of the FET by air pressure. Adapted with permission from Schaffhauser *et al.* [144] (Copyright © 2012 Public Library of Science). (Online version in colour.)

The two-electrode voltage clamping (TEVC) system is usually used to measure the membrane potential changes in *Xenopus* oocytes [142]. By downsizing this TEVC system and combining it with a fluidic channel, a compact fluidic device integrated with glass capillary electrodes was suggested as an odorant sensor using *Xenopus* oocyte expressing olfactory receptors [143]. In the suggested device, two oocytes expressing the receptor (BmOR1 or BmOR3) were serially arrayed in the fluidic channel, and the system identified the pheromones of bombykol or bombykal even in a mixture. Furthermore, it is notable that this cell-based sensor device could be mounted on a robotic system, and the robot motion synchronized the responses of *Xenopus* oocytes to an odorant stimulus. In this system, the insertion of electrodes into the oocyte shorten the lifespan of the sensor device, which is a limitation.

Other recent research studies have indicated that ion-sensitive FET (ISFET) could be useful for the detection of proton diffusion caused by some membrane transport proteins expressed in *Xenopus* oocytes [144]. The system based on ISFET is sensitive to decreases or increases in the concentration of hydrogen ions on the sensor surface. A stable contact between the cell surface and ion-sensitive membrane of the ISFET is required and, therefore, the *Xenopus* oocyte is pressed against the sensor surface by controlled pneumatic pressure (figure 9). The demonstrated membrane proteins were not olfactory receptors, and the system is a detecting device for membrane potential changes of a cell rather than a cell-based chemical sensor. However, this system is potentially useful as an odorant sensor using *Xenopus* oocytes expressing olfactory receptors because of its compact system and non-invasive cellular approach.

Xenopus oocytes have a uniform spherical shape in contrast to the general diversiform of cultivated cells. Therefore, bead array techniques [145] used in microfluidics are applicable to arranging a number of *Xenopus* oocytes and, thus, numerous oocytes would be useful for odorant sensor devices. One

drawback of this system is that individual oocytes require transformation with each preparation.

4. Outlook

On the lipid-bilayer-based platforms, the sensor elements developed to date are composed of single nanopores, with supplementary molecules in some cases. The principle of the sensor relies on the stochastic detection of analytes or probes by the pore; thus, it is challenging to use this platform for the quantitative detection of analytes at low concentrations [146,147]. On the other hand, it is advantageous that reproducible output signals with the same sensitivity and specificity can be expected between the individual assays since the sensor elements are consistently assembled in molecular level. Together with the development of synthetic nanopores, we consider that the comprehensive design of the lipid-bilayer platform is indispensable for biosensing applications [148], including the method of lipid bilayer formation, device configurations, electronics and software. Although numbers of the methods and devices have been reported, further development and improvement are required, especially for sensing devices such as usability, stability and portability [149–155]. Moreover, the integration of sensor elements on a single platform would allow performance of multiplex assays for detection of multiple target analytes and facilitate quantitative analyses [156–161].

In cell-based chemical sensors, there are differences in cellular responses to chemicals due to variations in protein expression level caused by cell cycle and individual cell variability. Therefore, it may be difficult to obtain quantitative and reproducible detection of target substances using single cell responses. For biosensors that use cells as senor elements, irrespective of whether a single cell or a population of cells is used, microchambers and microfluidic devices are the commonly used biosensing devices. For Sf cells, some studies indicate

that cellular responses to chemicals depend on the size of the culture space [162,163]. Thus, adequate cell arrangements would be required according to the applications. Practically, it is difficult to secure a constant space for cell growth because of their proliferation. Therefore, it is possible that cell-based sensors have an expiration date. In these respects, cell-based sensors are limited for use comparing with conventional inorganic material-based sensors.

For the detection of fluorescence from multiple cells that express different olfactory receptors, regionally selective placement of cells is principally used presently. The density of the cell arrangement pattern is expected to increase depending on the number of olfactory receptors. According to the high integration of cell patterning, increasing the imaging area and functional advancement of photodetectors would be required. In the system based on the electrical measurements of cells, transducers such as FET are suitable for integration. On the one hand, in the system based on measurements of cell membrane potential changes, multiplexing amplifiers are inevitable. Except for studies using spheroidal HEK cells [97], most research studies of cell-based odorant sensors presented here used detergent-solubilized odorous substances and not gaseous odorants as target samples. For the direct detection of airborne molecules from the atmosphere, there are few recent reports of the use of odorant-binding proteins [164,165]. In addition, to form the air–liquid interface near the cell surface, some studies suggest the use of collagen to encapsulate HEK cells and corneal epithelial cells as the host

cells for expressing olfactory receptors [166,167]. In the future, the development of efficient odorant solubilization systems that are benign for cells and olfactory receptors would be needed.

Membrane proteins are attractive materials for the development of biomimetic sensors, especially because of their specificity to the target substances. As reported in this review, numbers of works have proved the specificity that discriminated minor difference of molecular configurations, which could be difficult for traditional sensors. The mechanical robustness and lifetime of these sensors are particularly the challenging issues to be solved for practical applications, while the long-term storage could be possible by refrigeration. Although the variations of the membrane proteins reported so far are still limited, we expect that further studies would explore and discover the proteins available for versatile sensing applications.

References

1. Santos R *et al.* 2016 A comprehensive map of molecular drug targets. *Nat. Rev. Drug Discov.* **16**, 19–34. (doi:10.1038/nrd.2016.230)

2. Sato K, Pellegrino M, Nakagawa T, Nakagawa T, Vosshall LB, Touhara K. 2008 Insect olfactory receptors are heteromeric ligand-gated ion channels. *Nature* **452**, 1002–1006. (doi:10.1038/nature06850)

3. Wicher D, Schäfer R, Bauernfeind R, Stensmyr MC, Heller R, Heinemann SH, Hansson BS. 2008 *Drosophila* odorant receptors are both ligand-gated and cyclic-nucleotide-activated cation channels. *Nature* **452**, 1007–1011. (doi:10.1038/nature06861)

4. Spehr M, Munger SD. 2009 Olfactory receptors: G protein-coupled receptors and beyond. *J. Neurochem.* **109**, 1570–1583. (doi:10.1111/j.1471-4159.2009.06085.x)

5. Funakoshi K, Suzuki H, Takeuchi S. 2006 Lipid bilayer formation by contacting monolayers in a microfluidic device for membrane protein analysis. *Anal. Chem.* **78**, 8169–8174. (doi:10.1021/ac0613479)

6. Kawano R, Tsuji Y, Sato K, Osaki T, Kamiya K, Hirano M, Ide T, Miki N, Takeuchi S. 2013 Automated parallel recordings of topologically identified single ion channels. *Sci. Rep.* **3**, 1995. (doi:10.1038/srep01995)

7. Holden MA, Needham D, Bayley H. 2007 Functional bionetworks from nanoliter water droplets. *J. Am. Chem. Soc.* **129**, 8650–8655. (doi:10.1021/ja072292a)

8. Heron AJ, Thompson JR, Mason AE, Wallace MI. 2007 Direct detection of membrane channels from gels using water-in-oil droplet bilayers. *J. Am. Chem. Soc.* **129**, 16 042–16 047. (doi:10.1021/ja075715h)

9. Poulos JL, Jeon T-J, Damoiseaux R, Gillespie EJ, Bradley KA, Schmidt JJ. 2009 Ion channel and toxin measurement using a high throughput lipid membrane platform. *Biosens. Bioelectron.* **24**, 1806–1810. (doi:10.1016/j.bios.2008.08.041)

10. Czekalska MA, Kaminski TS, Jakiela S, Tanuj Sapra K, Bayley H, Garstecki P. 2015 A droplet microfluidic system for sequential generation of lipid bilayers and transmembrane electrical recordings. *Lab Chip* **15**, 541–548. (doi:10.1039/C4LC00985A)

11. Aghdaei S, Sandison ME, Zagnoni M, Green NG, Morgan H. 2008 Formation of artificial lipid bilayers using droplet dielectrophoresis. *Lab Chip* **8**, 1617. (doi:10.1039/b807374k)

12. Poulos JL, Nelson WC, Jeon T-J, Kim C-J, Schmidt JJ. 2009 Electrowetting on dielectric-based microfluidics for integrated lipid bilayer formation and measurement. *Appl. Phys. Lett.* **95**, 13706. (doi:10.1063/1.3167283)

13. Oshima A, Hirano-Iwata A, Mozumi H, Ishinari Y, Kimura Y, Niwano M. 2013 Reconstitution of human ether-a-go-go -related gene channels in microfabricated silicon chips. *Anal. Chem.* **85**, 4363–4369. (doi:10.1021/ac303484k)

14. Stimberg VC, Bomer JG, van Uitert I, van den Berg A, Le Gac S. 2013 High yield, reproducible and quasi-automated bilayer formation in a microfluidic format. *Small* **9**, 1076–1085. (doi:10.1002/smll.201201821)

15. Watanabe R *et al.* 2014 Arrayed lipid bilayer chambers allow single-molecule analysis of membrane transporter activity. *Nat. Commun.* **5**, 4519. (doi:10.1038/ncomms5519)

16. del Rio Martinez JM, Zaitseva E, Petersen S, Baaken G, Behrends JC. 2015 Automated formation of lipid membrane microarrays for ionic single-molecule sensing with protein nanopores. *Small* **11**, 119–125. (doi:10.1002/smll.201402016)

17. Robertson JWF, Rodrigues CG, Stanford VM, Rubinson KA, Krasilnikov OV, Kasianowicz JJ. 2007 Single-molecule mass spectrometry in solution using a solitary nanopore. *Proc. Natl Acad. Sci. USA* **104**, 8207–8211. (doi:10.1073/pnas.0611085104)

18. Song L, Hobaugh MR, Shustak C, Cheley S, Bayley H, Gouaux JE. 1996 Structure of staphylococcal alpha-hemolysin, a heptameric transmembrane pore. *Science* **274**, 1859–1865. (doi:10.1126/science.274.5294.1859)

19. Menestrina G. 1986 Ionic channels formed by Staphylococcus aureus alpha-toxin: voltage-dependent inhibition by divalent and trivalent

cations. *J. Membr. Biol.* **90**, 177–190. (doi:10.1007/BF01869935)

20. Baaken G, Halimeh I, Bacri L, Pelta J, Oukhaled A, Behrends JC. 2015 High-resolution size-discrimination of single nonionic synthetic polymers with a highly charged biological nanopore. *ACS Nano* **9**, 6443–6449. (doi:10.1021/acsnano.5b02096)

21. Pastoriza-Gallego M, Rabah L, Gibrat G, Thiebot B, van der Goot FG, Auvray L, Betton J-M, Pelta J. 2011 Dynamics of unfolded protein transport through an aerolysin pore. *J. Am. Chem. Soc.* **133**, 2923–2931. (doi:10.1021/ja1073245)

22. Stefureac R, Waldner L, Howard P, Lee JS. 2008 Nanopore analysis of a small 86-residue protein. *Small* **4**, 59–63. (doi:10.1002/smll.200700402)

23. Degiacomi MT, Iacovache I, Pernot L, Chami M, Kudryashev M, Stahlberg H, van der Goot FG, Dal Peraro M. 2013 Molecular assembly of the aerolysin pore reveals a swirling membrane-insertion mechanism. *Nat. Chem. Biol.* **9**, 623–629. (doi:10.1038/nchembio.1312)

24. Maglia G, Restrepo MR, Mikhailova E, Bayley H. 2008 Enhanced translocation of single DNA molecules through -hemolysin nanopores by manipulation of internal charge. *Proc. Natl. Acad. Sci. USA* **105**, 19 720–19 725. (doi:10.1073/pnas.0808296105)

25. Butler TZ, Gundlach JH, Troll M. 2007 Ionic current blockades from DNA and RNA molecules in the α-hemolysin nanopore. *Biophys. J.* **93**, 3229–3240. (doi:10.1529/biophysj.107.107003)

26. Clarke J, Wu H-C, Jayasinghe L, Patel A, Reid S, Bayley H. 2009 Continuous base identification for single-molecule nanopore DNA sequencing. *Nat. Nanotechnol.* **4**, 265–270. (doi:10.1038/nnano.2009.12)

27. Laszlo AH *et al.* 2014 Decoding long nanopore sequencing reads of natural DNA. *Nat. Biotechnol.* **32**, 829–833. (doi:10.1038/nbt.2950)

28. Stoddart D, Heron AJ, Mikhailova E, Maglia G, Bayley H. 2009 Single-nucleotide discrimination in immobilized DNA oligonucleotides with a biological nanopore. *Proc. Natl Acad. Sci. USA* **106**, 7702–7707. (doi:10.1073/pnas.0901054106)

29. Purnell RF, Schmidt JJ. 2009 Discrimination of single base substitutions in a DNA strand immobilized in a biological nanopore. *ACS Nano* **3**, 2533–2538. (doi:10.1021/nn900441x)

30. Derrington IM, Butler TZ, Collins MD, Manrao E, Pavlenok M, Niederweis M, Gundlach JH. 2010 Nanopore DNA sequencing with MspA. *Proc. Natl Acad. Sci. USA* **107**, 16 060–16 065. (doi:10.1073/pnas.1001831107)

31. Manrao EA, Derrington IM, Laszlo AH, Langford KW, Hopper MK, Gillgren N, Pavlenok M, Niederweis M, Gundlach JH. 2012 Reading DNA at single-nucleotide resolution with a mutant MspA nanopore and phi29 DNA polymerase. *Nat. Biotechnol.* **30**, 349–353. (doi:10.1038/nbt.2171)

32. Fuller CW *et al.* 2016 Real-time single-molecule electronic DNA sequencing by synthesis using polymer-tagged nucleotides on a nanopore array.

Proc. Natl Acad. Sci. USA **113**, 5233–5238. (doi:10.1073/pnas.1601782113)

33. Stranges PB *et al.* 2016 Design and characterization of a nanopore-coupled polymerase for single-molecule DNA sequencing by synthesis on an electrode array. *Proc. Natl Acad. Sci. USA* **113**, E6749–E6756. (doi:10.1073/pnas.1608271113)

34. Deamer D, Akeson M, Branton D. 2016 Three decades of nanopore sequencing. *Nat. Biotechnol.* **34**, 518–524. (doi:10.1038/nbt.3423)

35. Schmidt J. 2016 Membrane platforms for biological nanopore sensing and sequencing. *Curr. Opin. Biotechnol.* **39**, 17–27. (doi:10.1016/j.copbio.2015.12.015)

36. Laszlo AH, Derrington IM, Gundlach JH. 2016 MspA nanopore as a single-molecule tool: from sequencing to SPRNT. *Methods* **105**, 75–89. (doi:10.1016/j.ymeth.2016.03.026)

37. Bartel DP. 2004 MicroRNAs: genomics, biogenesis, mechanism, and function. *Cell* **116**, 281–297. (doi:10.1016/S0092-8674(04)00045-5)

38. Garzon R, Calin GA, Croce CM. 2009 MicroRNAs in cancer. *Annu. Rev. Med.* **60**, 167–179. (doi:10.1146/annurev.med.59.053006.104707)

39. Graybill RM, Bailey RC. 2016 Emerging biosensing approaches for microRNA analysis. *Anal. Chem.* **88**, 431–450. (doi:10.1021/acs.analchem.5b04679)

40. Wang Y, Zheng D, Tan Q, Wang MX, Gu L-Q. 2011 Nanopore-based detection of circulating microRNAs in lung cancer patients. *Nat. Nanotechnol.* **6**, 668–674. (doi:10.1038/nnano.2011.147)

41. Tian K, He Z, Wang Y, Chen S-J, Gu L-Q. 2013 Designing a polycationic probe for simultaneous enrichment and detection of microRNAs in a nanopore. *ACS Nano* **7**, 3962–3969. (doi:10.1021/nn305789z)

42. Wanunu M, Morrison W, Rabin Y, Grosberg AY, Meller A. 2010 Electrostatic focusing of unlabelled DNA into nanoscale pores using a salt gradient. *Nat. Nanotechnol.* **5**, 160–165. (doi:10.1038/nnano.2009.379)

43. Jeon B, Muthukumar M. 2014 Polymer capture by α-hemolysin pore upon salt concentration gradient. *J. Chem. Phys.* **140**, 15101. (doi:10.1063/1.4855075)

44. Jeon B, Muthukumar M. 2016 Electrostatic control of polymer translocation speed through α-hemolysin protein pore. *Macromolecules* **49**, 9132–9138. (doi:10.1021/acs.macromol.6b01663)

45. Wang Y, Tian K, Du X, Shi R, Gu L. 2017 Remote activation of a nanopore for high-performance genetic detection using a pH taxis-mimicking mechanism. *Anal. Chem.* **89**, 13 039–13 043. (doi:10.1021/acs.analchem.7b03979)

46. Ivica J, Williamson PTF, de Planque MRR. 2017 Salt gradient modulation of MicroRNA translocation through a biological nanopore. *Anal. Chem.* **89**, 8822–8829. (doi:10.1021/acs.analchem.7b01246)

47. Wang Y, Yao F, Kang X. 2015 Tetramethylammonium-filled protein nanopore for single-molecule analysis. *Anal. Chem.* **87**, 9991–9997. (doi:10.1021/acs.analchem.5b02611)

48. Gurnev PA, Roark TC, Petrache HI, Sodt AJ, Bezrukov SM. 2017 Cation-selective channel regulated by

anions according to their Hofmeister ranking. *Angew. Chemie Int. Ed.* **56**, 3506–3509. (doi:10.1002/anie.201611335)

49. Zhang H, Hiratani M, Nagaoka K, Kawano R. 2017 MicroRNA detection at femtomolar concentrations with isothermal amplification and a biological nanopore. *Nanoscale* **9**, 16 124–16 127. (doi:10.1039/C7NR04215A)

50. Natsume T, Ishikawa Y, Dedachi K, Tsukamoto T, Kurita N. 2007 Hybridization energies of double strands composed of DNA, RNA, PNA and LNA. *Chem. Phys. Lett.* **434**, 133–138. (doi:10.1016/j.cplett.2006.12.017)

51. Xi D, Shang J, Fan E, You J, Zhang S, Wang H. 2016 Nanopore-based selective discrimination of microRNAs with single-nucleotide difference using locked nucleic acid-modified probes. *Anal. Chem.* **88**, 10 540–10 546. (doi:10.1021/acs.analchem.6b02620)

52. Johnson RP, Fleming AM, Beuth LR, Burrows CJ, White HS. 2016 Base flipping within the α-Hemolysin latch allows single-molecule identification of mismatches in DNA. *J. Am. Chem. Soc.* **138**, 594–603. (doi:10.1021/jacs.5b10710)

53. Johnson RP, Fleming AM, Perera RT, Burrows CJ, White HS. 2017 Dynamics of a DNA mismatch site held in confinement discriminate epigenetic modifications of cytosine. *J. Am. Chem. Soc.* **139**, 2750–2756. (doi:10.1021/jacs.6b12284)

54. Zhang X, Wang Y, Fricke BL, Gu L. 2014 Programming nanopore ion flow for encoded multiplex microRNA detection. *ACS Nano* **8**, 3444–3450. (doi:10.1021/nn406339n)

55. Zhao Q, de Zoysa RSS, Wang D, Jayawardhana DA, Guan X. 2009 Real-time monitoring of peptide cleavage using a nanopore probe. *J. Am. Chem. Soc.* **131**, 6324–6325. (doi:10.1021/ja9004893)

56. Singh PR, Bárcena-Uribarri I, Modi N, Kleinekathöfer U, Benz R, Winterhalter M, Mahendran KR. 2012 Pulling peptides across nanochannels: resolving peptide binding and translocation through the hetero-oligomeric channel from Nocardia farcinica. *ACS Nano* **6**, 10 699–10 707. (doi:10.1021/nn303900y)

57. Nivala J, Marks DB, Akeson M. 2013 Unfoldase-mediated protein translocation through an α-hemolysin nanopore. *Nat. Biotechnol.* **31**, 247–250. (doi:10.1038/nbt.2503)

58. Rotem D, Jayasinghe L, Salichou M, Bayley H. 2012 Protein detection by nanopores equipped with aptamers. *J. Am. Chem. Soc.* **134**, 2781–2787. (doi:10.1021/ja2105653)

59. Celaya G, Perales-Calvo J, Muga A, Moro F, Rodriguez-Larrea D. 2017 Label-free, multiplexed, single-molecule analysis of protein–DNA complexes with nanopores. *ACS Nano* **11**, 5815–5825. (doi:10.1021/acsnano.7b01434)

60. Rauf S, Zhang L, Ali A, Ahmad J, Liu Y, Li J. 2017 Nanopore-based, label-free, and real-time monitoring assay for DNA methyltransferase activity and inhibition. *Anal. Chem.* **89**, 13252–13260. (doi:10.1021/acs.analchem.7b03278)

61. Cao C, Ying Y-L, Hu Z-L, Liao D-F, Tian H, Long Y-T. 2016 Discrimination of oligonucleotides of different

lengths with a wild-type aerolysin nanopore. *Nat. Nanotechnol.* **11**, 713–718. (doi:10.1038/nnano. 2016.66)

62. Yu J, Cao C, Long Y-T. 2017 Selective and sensitive detection of methylcytosine by aerolysin nanopore under serum condition. *Anal. Chem.* **89**, 11 685–11 689. (doi:10.1021/acs.analchem.7b03133)

63. Wang L, Han Y, Zhou S, Wang G, Guan X. 2014 Nanopore biosensor for label-free and real-time detection of anthrax lethal factor. *ACS Appl. Mater. Interfaces* **6**, 7334–7339. (doi:10.1021/am500749p)

64. Wang H-Y, Ying Y-L, Li Y, Kraatz H-B, Long Y-T. 2011 Nanopore analysis of β-amyloid peptide aggregation transition induced by small molecules. *Anal. Chem.* **83**, 1746–1752. (doi:10.1021/ac1029874)

65. Wang Y, Montana V, Grubišić V, Stout RF, Parpura V, Gu L-Q. 2015 Nanopore sensing of botulinum toxin type B by discriminating an enzymatically cleaved peptide from a synaptic protein synaptobrevin 2 derivative. *ACS Appl. Mater. Interfaces* **7**, 184–192. (doi:10.1021/am5056596)

66. Kawano R, Osaki T, Sasaki H, Takinoue M, Yoshizawa S, Takeuchi S. 2011 Rapid detection of a cocaine-binding aptamer using biological nanopores on a chip. *J. Am. Chem. Soc.* **133**, 8474–8477. (doi:10.1021/ja2026085)

67. Rauf S, Zhang L, Ali A, Liu Y, Li J. 2017 Label-free nanopore biosensor for rapid and highly sensitive cocaine detection in complex biological fluids. *ACS Sens.* **2**, 227–234. (doi:10.1021/acssensors.6b00627)

68. Fujii S, Nobukawa A, Osaki T, Morimoto Y, Kamiya K, Misawa N, Takeuchi S. 2017 Pesticide vapor sensing using an aptamer, nanopore, and agarose gel on a chip. *Lab Chip* **17**, 2421–2425. (doi:10.1039/C7LC00361G)

69. Guan X, Gu L-Q, Cheley S, Braha O, Bayley H. 2005 Stochastic sensing of TNT with a genetically engineered pore. *Chembiochem* **6**, 1875–1881. (doi:10.1002/cbic.200500064)

70. Wu H-C, Bayley H. 2008 Single-molecule detection of nitrogen mustards by covalent reaction within a protein nanopore. *J. Am. Chem. Soc.* **130**, 6813–6819. (doi:10.1021/ja8004607)

71. Gu L-Q, Braha O, Conlan S, Cheley S, Bayley H. 1999 Stochastic sensing of organic analytes by a pore-forming protein containing a molecular adapter. *Nature* **398**, 686–690. (doi:10.1038/19491)

72. Bayley H, Cremer PS. 2001 Stochastic sensors inspired by biology. *Nature* **413**, 226–230. (doi:10.1038/35093038)

73. Zhou J, Rossi J. 2016 Aptamers as targeted therapeutics: current potential and challenges. *Nat. Rev. Drug Discov.* **16**, 181–202. (doi:10.1038/nrd.2016.199)

74. Li T, Liu L, Li Y, Xie J, Wu H-C. 2015 A universal strategy for aptamer-based nanopore sensing through host-guest interactions inside α-hemolysin. *Angew. Chemie Int. Ed.* **54**, 7568–7571. (doi:10.1002/anie.201502047)

75. Capone R, Blake S, Rincon Restrepo M, Yang J, Mayer M. 2007 Designing nanosensors based on charged derivatives of gramicidin A. *J. Am. Chem. Soc.* **129**, 9737–9745. (doi:10.1021/ja0711819)

76. Macrae MX, Blake S, Jiang X, Capone R, Estes DJ, Mayer M, Yang J. 2009 A semi-synthetic ion channel platform for detection of phosphatase and protease activity. *ACS Nano* **3**, 3567–3580. (doi:10.1021/nn901231h)

77. Su G, Zhang M, Si W, Li Z, Hou J. 2016 Directional potassium transport through a unimolecular peptide channel. *Angew. Chemie Int. Ed.* **55**, 14 678–14 682. (doi:10.1002/anie.201608428)

78. Burns JR, Stulz E, Howorka S. 2013 Self-assembled DNA nanopores that span lipid bilayers. *Nano Lett.* **13**, 2351–2356. (doi:10.1021/nl304147f)

79. Burns JR, Seifert A, Fertig N, Howorka S. 2016 A biomimetic DNA-based channel for the ligand-controlled transport of charged molecular cargo across a biological membrane. *Nat. Nanotechnol.* **11**, 152–156. (doi:10.1038/nnano.2015.279)

80. Langecker M, Arnaut V, Martin TG, List J, Renner S, Mayer M, Dietz H, Simmel FC. 2012 Synthetic lipid membrane channels formed by designed DNA nanostructures. *Science* **338**, 932–936. (doi:10.1126/science.1225624)

81. Krishnan S, Ziegler D, Arnaut V, Martin TG, Kapsner K, Henneberg K, Bausch AR, Dietz H, Simmel FC. 2016 Molecular transport through large-diameter DNA nanopores. *Nat. Commun.* **7**, 12787. (doi:10.1038/ncomms12787)

82. Jung M, Kim H, Baek K, Kim K. 2008 Synthetic ion channel based on metal–organic polyhedra. *Angew. Chemie Int. Ed.* **47**, 5755–5757. (doi:10.1002/anie.200802240)

83. Kulikov OV, Li R, Gokel GW. 2009 A synthetic ion channel derived from a metallogallarene capsule that functions in phospholipid bilayers. *Angew. Chemie Int. Ed.* **48**, 375–377. (doi:10.1002/anie.200804099)

84. Kawano R *et al.* 2017 Metal-organic cuboctahedra for synthetic ion channels with multiple conductance states. *Chem* **2**, 393–403. (doi:10.1016/j.chempr.2017.02.002)

85. Muraoka T, Umetsu K, Tabata KV, Hamada T, Noji H, Yamashita T, Kinbara K. 2017 Mechano-sensitive synthetic ion channels. *J. Am. Chem. Soc.* **139**, 18 016–18 023. (doi:10.1021/jacs.7b09515)

86. Liu L, Yang C, Zhao K, Li J, Wu H-C. 2013 Ultrashort single-walled carbon nanotubes in a lipid bilayer as a new nanopore sensor. *Nat. Commun.* **4**, 2989. (doi:10.1038/ncomms3989)

87. Geng J *et al.* 2014 Stochastic transport through carbon nanotubes in lipid bilayers and live cell membranes. *Nature* **514**, 612–615. (doi:10.1038/nature13817)

88. Yusko EC, Johnson JM, Majd S, Prangkio P, Rollings RC, Li J, Yang J, Mayer M. 2011 Controlling protein translocation through nanopores with bio-inspired fluid walls. *Nat. Nanotechnol.* **6**, 253–260. (doi:10.1038/nnano.2011.12)

89. Yusko EC *et al.* 2016 Real-time shape approximation and fingerprinting of single proteins using a nanopore. *Nat. Nanotechnol.* **12**, 360–367. (doi:10.1038/nnano.2016.267)

90. Rawson DM, Willmer AJ, Turner APP. 1989 Whole-cell biosensors for environmental monitoring. *Biosensors* **4**, 299–311. (doi:10.1016/0265-928X(89)80011-2)

91. King JMH, DiGrazia PM, Applegate B, Burlage R, Sanseverino J, Dunbar P, Larimer F, Sayler GS. 1990 Rapid, sensitive bioluminescent reporter technology for naphthalene exposure and biodegradation. *Science* **249**, 778–781. (doi:10.1126/science.249.4970.778)

92. Shear J, Fishman H, Allbritton N, Garigan D, Zare R, Scheller R. 1995 Single cells as biosensors for chemical separations. *Science* **267**, 74–77. (doi:10.1126/science.7809609)

93. Bousse L. 1996 Whole cell biosensors. *Sens. Actuators B Chem.* **34**, 270–275. (doi:10.1016/S0925-4005(96)01906-5)

94. Stenger DA, Gross GW, Keefer EW, Shaffer KM, Andreadis JD, Ma W, Pancrazio JJ. 2001 Detection of physiologically active compounds using cell-based biosensors. *Trends Biotechnol.* **19**, 304–309. (doi:10.1016/S0167-7799(01)01690-0)

95. Ko HJ, Park TH. 2016 Bioelectronic nose and its application to smell visualization. *J. Biol. Eng.* **10**, 17. (doi:10.1186/s13036-016-0041-4)

96. Figueroa XA, Cooksey GA, Votaw SV, Horowitz LF, Folch A. 2010 Large-scale investigation of the olfactory receptor space using a microfluidic microwell array. *Lab Chip* **10**, 1120. (doi:10.1039/b920585c)

97. Sato K, Takeuchi S. 2014 Chemical vapor detection using a reconstituted insect olfactory receptor complex. *Angew. Chemie Int. Ed.* **53**, 11 798–11 802. (doi:10.1002/anie.201404720)

98. Termtanasombat M, Mitsuno H, Misawa N, Yamahira S, Sakurai T, Yamaguchi S, Nagamune T, Kanzaki R. 2016 Cell-based odorant sensor array for odor discrimination based on insect odorant receptors. *J. Chem. Ecol.* **42**, 716–724. (doi:10.1007/s10886-016-0726-7)

99. Takeuchi H, Sakano H. 2014 Neural map formation in the mouse olfactory system. *Cell. Mol. Life Sci.* **71**, 3049–3057. (doi:10.1007/s00018-014-1597-0)

100. Barish S, Volkan PC. 2015 Mechanisms of olfactory receptor neuron specification in *Drosophila*. *Wiley Interdiscip. Rev. Dev. Biol.* **4**, 609–621. (doi:10.1002/wdev.197)

101. Park KC. 2002 Odor discrimination using insect electroantennogram responses from an insect antennal array. *Chem. Senses* **27**, 343–352. (doi:10.1093/chemse/27.4.343)

102. Liu Q, Ye W, Yu H, Hu N, Du L, Wang P, Yang M. 2010 Olfactory mucosa tissue-based biosensor: a bioelectronic nose with receptor cells in intact olfactory epithelium. *Sens. Actuators B Chem.* **146**, 527–533. (doi:10.1016/j.snb.2009.12.032)

103. Liu Q, Ye W, Xiao L, Du L, Hu N, Wang P. 2010 Extracellular potentials recording in intact olfactory epithelium by microelectrode array for a bioelectronic nose. *Biosens. Bioelectron.* **25**, 2212–2217. (doi:10.1016/j.bios.2010.02.024)

104. Liu Q, Ye W, Hu N, Cai H, Yu H, Wang P. 2010 Olfactory receptor cells respond to odors in a tissue

and semiconductor hybrid neuron chip. *Biosens. Bioelectron.* **26**, 1672–1678. (doi:10.1016/j.bios.2010.09.019)

105. Chen Q, Xiao L, Liu Q, Ling S, Yin Y, Dong Q, Wang P. 2011 An olfactory bulb slice-based biosensor for multi-site extracellular recording of neural networks. *Biosens. Bioelectron.* **26**, 3313–3319. (doi:10.1016/j.bios.2011.01.005)

106. Liu Q, Hu N, Zhang F, Zhang D, Hsia KJ, Wang P. 2012 Olfactory epithelium biosensor: odor discrimination of receptor neurons from a bio-hybrid sensing system. *Biomed. Microdevices* **14**, 1055–1061. (doi:10.1007/s10544-012-9705-0)

107. Tanada N, Sakurai T, Mitsuno H, Bakkum DJ, Kanzaki R, Takahashi H. 2012 Dissociated neuronal culture expressing ionotropic odorant receptors as a hybrid odorant biosensor—proof-of-concept study. *Analyst* **137**, 3452. (doi:10.1039/c2an35058k)

108. Huotari MJ. 2000 Biosensing by insect olfactory receptor neurons. *Sens. Actuators B Chem.* **71**, 212–222. (doi:10.1016/S0925-4005(00)00619-5)

109. Huotari M, Lantto V. 2007 Measurements of odours based on response analysis of insect olfactory receptor neurons. *Sens. Actuators B Chem.* **127**, 284–287. (doi:10.1016/j.snb.2007.07.055)

110. Corcelli A, Lobasso S, Lopalco P, Dibattista M, Araneda R, Peterlin Z, Firestein S. 2010 Detection of explosives by olfactory sensory neurons. *J. Hazard. Mater.* **175**, 1096–1100. (doi:10.1016/j.jhazmat.2009.10.054)

111. Ling S *et al.* 2010 The fabrication of an olfactory receptor neuron chip based on planar multi-electrode array and its odor-response analysis. *Biosens. Bioelectron.* **26**, 1124–1128. (doi:10.1016/j.bios.2010.08.071)

112. Liu Q, Cai H, Xu Y, Li Y, Li R, Wang P. 2006 Olfactory cell-based biosensor: a first step towards a neurochip of bioelectronic nose. *Biosens. Bioelectron.* **22**, 318–322. (doi:10.1016/j.bios.2006.01.016)

113. Wu C, Chen P, Yu H, Liu Q, Zong X, Cai H, Wang P. 2009 A novel biomimetic olfactory-based biosensor for single olfactory sensory neuron monitoring. *Biosens. Bioelectron.* **24**, 1498–1502. (doi:10.1016/j.bios.2008.07.065)

114. Datta-Chaudhuri T, Araneda RC, Abshire P, Smela E. 2016 Olfaction on a chip. *Sens. Actuators B Chem.* **235**, 74–78. (doi:10.1016/j.snb.2016.05.048)

115. Russell WC, Graham FL, Smiley J, Nairn R. 1977 Characteristics of a human cell line transformed by DNA from human adenovirus type 5. *J. Gen. Virol.* **36**, 59–72. (doi:10.1099/0022-1317-36-1-59)

116. Shaw G. 2002 Preferential transformation of human neuronal cells by human adenoviruses and the origin of HEK 293 cells. *FASEB J.* **16**, 869–871. (doi:10.1096/fj.01-0995fje)

117. Thomas P, Smart TG. 2005 HEK293 cell line: a vehicle for the expression of recombinant proteins. *J. Pharmacol. Toxicol. Methods* **51**, 187–200. (doi:10.1016/j.vascn.2004.08.014)

118. Ko HJ, Park TH. 2005 Piezoelectric olfactory biosensor: ligand specificity and dose-dependence of an olfactory receptor expressed in a heterologous cell system. *Biosens. Bioelectron.* **20**, 1327–1332. (doi:10.1016/j.bios.2004.05.002)

119. Ko HJ, Park TH. 2007 Functional analysis of olfactory receptors expressed in a HEK-293 cell system by using cameleons. *J. Microbiol. Biotechnol.* **17**, 928–933.

120. Lee SH, Jun SB, Ko HJ, Kim SJ, Park TH. 2009 Cell-based olfactory biosensor using microfabricated planar electrode. *Biosens. Bioelectron.* **24**, 2659–2664. (doi:10.1016/j.bios.2009.01.035)

121. Lee SH, Jeong SH, Jun SB, Kim SJ, Park TH. 2009 Enhancement of cellular olfactory signal by electrical stimulation. *Electrophoresis* **30**, 3283–3288. (doi:10.1002/elps.200900124)

122. Lee SH, Ko HJ, Park TH. 2009 Real-time monitoring of odorant-induced cellular reactions using surface plasmon resonance. *Biosens. Bioelectron.* **25**, 55–60. (doi:10.1016/j.bios.2009.06.007)

123. Oh EH, Lee SH, Lee SH, Ko HJ, Park TH. 2014 Cell-based high-throughput odorant screening system through visualization on a microwell array. *Biosens. Bioelectron.* **53**, 18–25. (doi:10.1016/j.bios.2013.09.039)

124. Mortimer RK, Johnston JR. 1986 Genealogy of principal strains of the yeast genetic stock center. *Genetics* **113**, 35–43.

125. Greig D, Leu J-Y. 2009 Natural history of budding yeast. *Curr. Biol.* **19**, R886–R890. (doi:10.1016/j.cub.2009.07.037)

126. Mortimer RK. 2000 Evolution and variation of the yeast (*Saccharomyces*) genome. *Genome Res.* **10**, 403–409. (doi:10.1101/gr.10.4.403)

127. Duina AA, Miller ME, Keeney JB. 2014 Budding yeast for budding geneticists: a primer on the Saccharomyces cerevisiae model system. *Genetics* **197**, 33–48. (doi:10.1534/genetics.114.163188)

128. Pajot-Augy E, Crowe M, Levasseur G, Salesse R, Connerton I. 2003 Engineered yeasts as reporter systems for odorant detection. *J. Recept. Signal Transduct.* **23**, 155–171. (doi:10.1081/RRS-120025196)

129. Minic J, Persuy M-A, Godel E, Aioun J, Connerton I, Salesse R, Pajot-Augy E. 2005 Functional expression of olfactory receptors in yeast and development of a bioassay for odorant screening. *FEBS J.* **272**, 524–537. (doi:10.1111/j.1742-4658.2004.04494.x)

130. Radhika V, Proikas-Cezanne T, Jayaraman M, Onesime D, Ha JH, Dhanasekaran DN. 2007 Chemical sensing of DNT by engineered olfactory yeast strain. *Nat. Chem. Biol.* **3**, 325–330. (doi:10.1038/nchembio882)

131. Fukutani Y, Hori A, Tsukada S, Sato R, Ishii J, Kondo A, Matsunami H, Yohda M. 2015 Improving the odorant sensitivity of olfactory receptor-expressing yeast with accessory proteins. *Anal. Biochem.* **471**, 1–8. (doi:10.1016/j.ab.2014.10.012)

132. Marrakchi M, Vidic J, Jaffrezic-Renault N, Martelet C, Pajot-Augy E. 2007 A new concept of olfactory biosensor based on interdigitated microelectrodes and immobilized yeasts expressing the human receptor OR17-40. *Eur. Biophys. J.* **36**, 1015–1018. (doi:10.1007/s00249-007-0187-6)

133. Sakurai T. 2014 Molecular and neural mechanisms of sex pheromone reception and processing in the silkmoth Bombyx mori. *Front. Physiol.* **5**, 1–20. (doi:10.3389/fphys.2014.00125)

134. Mombaerts P. 2004 Genes and ligands for odorant, vomeronasal and taste receptors. *Nat. Rev. Neurosci.* **5**, 263–278. (doi:10.1038/nrn1365)

135. DeMaria S, Ngai J. 2010 The cell biology of smell. *J. Cell Biol.* **191**, 443–452. (doi:10.1083/jcb.201008163)

136. Vaughn JL, Goodwin RH, Tompkins GJ, McCawley P. 1977 The establishment of two cell lines from the insect spodoptera frugiperda (*lepidoptera; noctuidae*). *In Vitro* **13**, 213–217. (doi:10.1007/BF02615077)

137. Mitsuno H, Sakurai T, Namiki S, Mitsuhashi H, Kanzaki R. 2015 Novel cell-based odorant sensor elements based on insect odorant receptors. *Biosens. Bioelectron.* **65**, 287–294. (doi:10.1016/j.bios.2014.10.026)

138. Terutsuki D, Mitsuno H, Okamoto Y, Sakurai T, Tixier-mita A. 2017 *Odor-sensitive field effect transistor (OSFET) based on insect cells expressing insect odorant receptors. Proc. IEEE Int. Conf. Micro Electro Mech. Syst., Las Vegas, NV, 22–26 January*, pp. 394–397. Piscataway, NJ: IEEE. (doi:10.1109/MEMSYS.2017.7863424)

139. Sigel E. 1990 Use of Xenopus oocytes for the functional expression of plasma membrane proteins. *J. Membr. Biol.* **117**, 201–221. (doi:10.1007/BF01868451)

140. Sigel E, Minier F. 2005 The Xenopus oocyte: System for the study of functional expression and modulation of proteins. *Mol. Nutr. Food Res.* **49**, 228–234. (doi:10.1002/mnfr.200400104)

141. Dahmen N, Wang H-L, Margolis FL. 1992 Expression of olfactory receptors in Xenopus oocytes. *J. Neurochem.* **58**, 1176–1179. (doi:10.1111/j.1471-4159.1992.tb09379.x)

142. Stühmer W. 1992 Electrophysiological recording from Xenopus oocytes. *Methods Enzymol.* **207**, 319–339. (doi:10.1016/0076-6879(92)07021-F)

143. Misawa N, Mitsuno H, Kanzaki R, Takeuchi S. 2010 Highly sensitive and selective odorant sensor using living cells expressing insect olfactory receptors. *Proc. Natl Acad. Sci. USA* **107**, 15 340–15 344. (doi:10.1073/pnas.1004334107)

144. Schaffhauser DF, Patti M, Goda T, Miyahara Y, Forster IC, Dittrich PS. 2012 An integrated field-effect microdevice for monitoring membrane transport in Xenopus laevis oocytes via lateral proton diffusion. *PLoS ONE* **7**, e39238. (doi:10.1371/journal.pone.0039238)

145. Nilsson J, Evander M, Hammarström B, Laurell T. 2009 Review of cell and particle trapping in microfluidic systems. *Anal. Chim. Acta* **649**, 141–157. (doi:10.1016/j.aca.2009.07.017)

146. Höfler L, Gyurcsányi RE. 2012 Nanosensors lost in space. A random walk study of single molecule detection with single-nanopore sensors. *Anal. Chim. Acta* **722**, 119–126. (doi:10.1016/j.aca.2012.02.010)

147. Agasid MT, Comi TJ, Saavedra SS, Aspinwall CA. 2017 Enhanced temporal resolution with ion

channel-functionalized sensors using a conductance-based measurement protocol. *Anal. Chem.* **89**, 1315 – 1322. (doi:10.1021/acs.analchem.6b04226)

148. Osaki T, Takeuchi S. 2017 Artificial cell membrane systems for biosensing applications. *Anal. Chem.* **89**, 216 – 231. (doi:10.1021/acs.analchem.6b04744)

149. Bright LK, Baker CA, Agasid MT, Ma L, Aspinwall CA. 2013 Decreased aperture surface energy enhances electrical, mechanical, and temporal stability of suspended lipid membranes. *ACS Appl. Mater. Interfaces* **5**, 11 918 – 11 926. (doi:10.1021/am403605h)

150. Kawano R, Osaki T, Sasaki H, Takeuchi S. 2010 A polymer-based nanopore-integrated microfluidic device for generating stable bilayer lipid membranes. *Small* **6**, 2100 – 2104. (doi:10.1002/smll.201000997)

151. Shim JW, Gu LQ. 2007 Stochastic sensing on a modular chip containing a single-ion channel. *Anal. Chem.* **79**, 2207 – 2213. (doi:10.1021/ac0614285)

152. Jeon T-J, Poulos JL, Schmidt JJ. 2008 Long-term storable and shippable lipid bilayer membrane platform. *Lab Chip* **8**, 1742. (doi:10.1039/b807932c)

153. Kang X, Cheley S, Rice-Ficht AC, Bayley H. 2007 A storable encapsulated bilayer chip containing a single protein nanopore. *J. Am. Chem. Soc.* **129**, 4701 – 4705. (doi:10.1021/ja068654g)

154. Jung S-H, Choi S, Kim Y-R, Jeon T-J. 2012 Storable droplet interface lipid bilayers for cell-free ion channel studies. *Bioprocess Biosyst. Eng.* **35**, 241 – 246. (doi:10.1007/s00449-011-0602-3)

155. Venkatesan GA, Sarles SA. 2016 Droplet immobilization within a polymeric organogel improves lipid bilayer durability and portability. *Lab Chip* **16**, 2116 – 2125. (doi:10.1039/C6LC00391E)

156. Osaki T, Suzuki H, Le Pioufle B, Takeuchi S. 2009 Multichannel simultaneous measurements of single-molecule translocation in α-hemolysin nanopore array. *Anal. Chem.* **81**, 9866 – 9870. (doi:10.1021/ac901732z)

157. Zagnoni M, Sandison ME, Morgan H. 2009 Microfluidic array platform for simultaneous lipid bilayer membrane formation. *Biosens. Bioelectron.* **24**, 1235 – 1240. (doi:10.1016/j.bios.2008.07.022)

158. Tsuji Y, Kawano R, Osaki T, Kamiya K, Miki N, Takeuchi S. 2013 Droplet split-and-contact method for high-throughput transmembrane electrical recording. *Anal. Chem.* **85**, 10 913 – 10 919. (doi:10.1021/ac402299z)

159. Tomoike F, Tonooka T, Osaki T, Takeuchi S. 2016 Repetitive formation of optically-observable planar lipid bilayers by rotating chambers on a microaperture. *Lab Chip* **16**, 2423 – 2426. (doi:10.1039/C6LC00363J)

160. Barlow NE, Bolognesi G, Flemming AJ, Brooks NJ, Barter LMC, Ces O. 2016 Multiplexed droplet Interface bilayer formation. *Lab Chip* **16**, 4653 – 4657. (doi:10.1039/C6LC01011C)

161. Lazenby RA, Macazo FC, Wormsbecher RF, White RJ. 2017 Quantitative framework for stochastic nanopore sensors using multiple channels. *Anal. Chem.* **90**, 903 – 911. (doi:10.1021/acs.analchem.7b03845)

162. Walker GM, Ozers MS, Beebe DJ. 2002 Insect cell culture in microfluidic channels. *Biomed. Microdevices* **4**, 161 – 166. (doi:10.1023/A:1016088128057)

163. Yu H, Meyvantsson I, Shkel IA, Beebe DJ. 2005 Diffusion dependent cell behavior in microenvironments. *Lab Chip* **5**, 1089. (doi:10.1039/b504403k)

164. Sankaran S, Panigrahi S, Mallik S. 2011 Odorant binding protein based biomimetic sensors for detection of alcohols associated with Salmonella contamination in packaged beef. *Biosens. Bioelectron.* **26**, 3103 – 3109. (doi:10.1016/j.bios.2010.07.122)

165. Larisika M *et al.* 2015 Electronic olfactory sensor based on A. mellifera odorant-binding protein 14 on a reduced graphene oxide field-effect transistor. *Angew. Chemie Int. Ed.* **54**, 13 245 – 13 248. (doi:10.1002/anie.201505712)

166. Hirata Y, Morimoto Y, Nam E, Yoshida S, Takeuchi S. 2017 *Cells smell on a CMOS: A portable odorant detection system using cell-laden collagen pillars*. *Proc. IEEE Int. Conf. Micro Electro Mech. Syst., Las Vegas, NV, 22 – 26 January*, pp. 13 – 16. Piscataway, NJ: IEEE. (doi:10.1109/MEMSYS.2017.7863327)

167. Nam E, Takeuchi S. 2017 *Volatile Odorant Detection By Corneal Epithelial Cells. Proc. IEEE Int. Conf. Micro Electro Mech. Syst., Las Vegas, NV, 22 – 26 January*, pp. 412 – 413. Piscataway, NJ: IEEE. (doi:10.1109/MEMSYS.2017.7863429)